Exosome Prevention of Post Operative Atrial Fibrillation

Sandrine Parent, B.Sc.

Thesis submitted to the University of Ottawa

in partial Fulfillment of the requirements for

the Master of Science degree.

Department of Cellular and Molecular Medicine

Faculty of Medicine

University of Ottawa

Supervisor: Darryl R. Davis, MD

Table of Contents

Acknowledgements

I would like to recognize and thank the following individuals for their contributions to this thesis:

Thesis Advisory Committee:

- Dr. Erik J Suuronen and Dr. Duncan J Stewart

Cardiac Translational Research Laboratory Members:

- Pushpinder Kanda, Melanie Villanueva, Ghazaleh Rafatian, Connor Michie and Bin Ye

University of Ottawa Heart Institute: Animal Care and Veterinary Services

University of Ottawa Heart Institute Cardiovascular Research Methods Centre: Study design, sample size calculations and analysis of the primary outcome.

University of Ottawa Louise Pelletier Histology Core Facility

Study Collaborators:

- Surgical staff at the University of Ottawa Heart Institute: Dr. Buu-Khanh Lam, Dr. Marc Ruel, Dr. Munir Boodhwani, Dr. Vincent Chan, and Dr. Fraser Rubens.

A special thank you to Richard Seymour, who performed all animal surgeries for this project. Without you, none of this work would've been possible.

I would also like to express my profound gratitude to my supervisor Dr. Darryl R Davis for his unfailing support, insight and continuous encouragement throughout the course of my studies.

This accomplishment would not have been possible without the above-mentioned individuals.

Sources of Funding

This project was supported by the Canadian Institutes of Health Research Project Grant 410103 and the Natural Sciences and Engineering Research Council of Canada (CHRPJ 549626 – 20 and I2IPJ 571244 – 22).

Conflicts of Interest Statement

Sandrine Parent and Darryl R Davis are co-inventors for a patent application submitted regarding extracellular vesicle treatment of atrial fibrillation (US patent filing number 63/278,518, Compositions of human heart derived extracellular vesicles and uses thereof).

Darryl R Davis, Sandrine Parent and Stanley Nattel are co-inventors for a patent application submitted regarding genetic modification of producer cell lines for extracellular vesicles (US patent 62758160, Engineered cardiac-derived stem cells and extracellular vesicles secreted by such cells, methods of preparing, and uses thereof).

David Courtman, Duncan J Stewart and Darryl R Davis hold a patent regarding serum-free and xenogen-free human cardiac explant-derived stem cells (US patent 11083756, Serum-free and xenogen-free human cardiac explant-derived stem cells and uses and methods for the production thereof).

Abstract

Almost half of patients recovering from open chest surgery experience atrial fibrillation (AF) that results principally from inflammation in the pericardial space surrounding the heart. Given that post-operative AF is associated with increased mortality, effective measures to prevent AF after open-chest surgery are highly desirable. In this study, we tested the concept that extracellular vesicles (EVs) isolated from human atrial explant-derived cells can prevent post-operative AF. Middle-aged female and male rats were randomized to undergo sham operation or induction of sterile pericarditis followed by trans-epicardial injection of human EVs or vehicle into the atrial tissue. Pericarditis increased the probability of inducing AF while EV treatment abrogated this effect in a sex independent manner. EV treatment reduced infiltration of inflammatory cells and production of pro-inflammatory cytokines. Atrial fibrosis and hypertrophy seen after pericarditis was markedly attenuated by EV pre-treatment; an effect attributable to suppression of fibroblast proliferation by EVs. Our study demonstrates that injection of extracellular vesicles at the time of open-chest surgery shows prominent anti-inflammatory effects and prevents AF due to sterile pericarditis. Translation of this finding to patients might provide an effective new strategy to prevent post-operative AF by reducing atrial inflammation and fibrosis.

List of Tables

List of Figures

List of Abbreviations

AF	Atrial fibrillation
APC	Aphidicolin
ANOVA	Analysis of variance
AVERP	Atrioventricular nodal refractory period
DAPI	4′, 6-diamidino-2-phenylindole
DMEM	Dulbecco's Modified Eagle Medium
ECM	Extracellular matrix
EDC	Explant derived cells
EDTA	Ethylenediaminetetraacetic acid
EdU	5-ethynyl-2´-deoxyuridine
ELISA	Enzyme-linked immunosorbent assay
EPS	Electrophysiological study
EV	Extracellular vesicle
FBS	Fetal bovine serum
FDR	False discovery rate
GMP	Grade manufacturing practice
HBSS	Hank's balanced salt solution

HPF	High power field
IL1β	Interleukin 1 beta
IL2	Interleukin 2
IL6	Interleukin 6
IL18	Interleukin 18
LFQ	Label-free quantification
MMP2	Matrix metalloprotein 2
OCT	Optimal cutting temperature
PBS	Phosphate-buffered saline
PE	Phycoerythrin
PFA	Paraformaldehyde
MCP1	Monocyte chemoattractant protein 1
MESF	Molecules of Equivalent Soluble Fluorochrome
miR	microRNA
PDGF-AB	Platelet-derived growth factor-AB
POAF	Post-operative atrial fibrillation
SEM	Standard error of the mean
TGFβ1	Transforming growth factor beta 1

TNFα	Tumour necrosis factor alpha
Veh	Vehicle

1.0 INTRODUCTION

Atrial fibrillation (AF) is the most common heart rhythm disturbance in the world-afflicting almost 38 million patients worldwide.[1-3] Although not usually acutely life threatening, AF can significantly impact the quality of life for an otherwise healthy patient by causing dizziness, fatigue, palpitations, and even syncope; and is associated with increased mortality, heart-failure risk, and stroke. For patients recovering from open-chest surgery on the heart or lungs, new onset post-operative AF (POAF) can be difficult to manage as many of the standard therapies (such as antiarrhythmics or anticoagulants) are contraindicated and routine post-operative medications (such as inotropes or vasopressors) increase the risk of AF, while complicating its management. It is thus unsurprising that new-onset POAF impacts surgical outcomes by increasing mortality, the length of inpatient stay, and overall procedural costs.[4,5] Given that almost half of all patients experience AF after cardiac surgery, regimes to prevent or treat POAF are highly desirable.[6]

There is at present no effective solution to prevent POAF.[7] Rhythm or rate control medications often fail and are limited by off-target effects on blood pressure or heart function.[8,9] Anti-inflammatory medications increase the risk of hyperglycemia, infection, gastritis, and myelosuppression.[10,11] Anti-fibrotic approaches similarly impact post-operative healing and increase the risk of infection.[12,13] Given these considerations, recent preclinical work has focused on biological therapies to reduce inflammation or modify atrial electrophysiology. Despite promising results in animal models, no biological therapy has been translated to the clinic because of poor-quality evidence, modest efficacy, the impractical nature of the intervention or the potential for complications.

Accordingly, we built on previous work from our group using human heart explant-derived cells (EDCs) to establish the potential value of extracellular vesicles (EVs), which mediate the

anti-fibrotic, anti-inflammatory effects of transplanted cells, for the prevention of POAF. EDCs are $CD105^{+}CD45^{-}$ cardiac-derived cells cultured from human atrial appendage biopsies obtained at the time of open-chest surgery. EDCs cultured in a GMP cell manufacturing facility using serum-free xenogen-free culture methods can be rapidly expanded to substantial doses (100M+ cells in 2-3 weeks) that provide large amounts of EVs rich in microRNAs associated with attenuation of adverse cardiac fibrosis/remodeling and inflammation.

EVs are lipid enclosed microparticles that range in size from 50 to 150 nm.[14] They are released from the membrane of cells by budding off and contain transcripts, proteins, and miRNA that mediate cell-to-cell signaling to influence tissue function.[14-16] Physiologically, EVs merge with and release their contents (mainly miRNAs) into neighboring cells to influence cell function.[16-18] EVs can be characterized by their distinct cell surface marker expression. Due to their endocytic origin, EVs are commonly enriched in proteins such as SNAREs, Annexins, and flotillin. Alix and Tsg101, as well as tetraspanins, like CD63, CD81 and CD9, are abundant in EVs and considered to be markers of true EV identity. Less is known about the protein identity of EVs, but common protein markers used to identify EVs are selectins, integrins and CD40 ligand.[19]

In this report, we evaluated whether EVs collected from EDC producer cell lines can suppress atrial fibrosis, atrial inflammation, and AF-promotion in a validated rodent model of post-operative sterile pericarditis.[20]

2.0 STUDY RATIONALE, AIM & HYPOTHESIS

2.1 Study rationale

Post-operative atrial fibrillation (POAF) is an important source of morbidity and mortality in Canada and the world. Over the past 10 years novel therapeutic strategies that rely upon EVs generated from heart explant-derived cells (EDCs) have been developed. EVs are vesicles created and released from the membrane of many, if not all, cells of the body. These fluid-filled sacs contain nucleic acids and proteins that participate in cell-to-cell signalling. Physiologically, secreted EVs merge with and release their contents into neighboring cells to influence cell function. For several years, it has been recognized that the cell origin-specific payloads within EVs mediate the therapeutic bioactivity for a wide variety of stem cell types, including EDCs cultured from atrial tissue.[21-26] Because they originate from the heart and provide a functionally superior paracrine product,[21] EDC EVs represent a logical candidate to repair the injured heart. The fundamental rationale of our approach is simple: ex vivo isolation and purification of EVs, followed by delivery to the atria during open-chest surgery, where they will reduce inflammation and prevent POAF. This proposal aims to develop a truly effective cell-free approach for the treatment of post-operative atrial fibrillation by addressing the key barriers encountered by previous efforts.

2.2 Research aim

To evaluate the ability of human EDC EVs to reduce the incidence of post-operative atrial fibrillation after open chest surgery in a rat model of sterile pericarditis.

2.3 Hypothesis

Injection of human EDC EVs into the left atrial wall of pericarditis rats will reduce atrial fibrosis and AF inducibility by reducing local inflammation and the malignant pro-fibrillatory transformation of atrial fibroblasts with no signal for adverse events.

3.0 MATERIALS & METHODS

3.1 Cell culture and EV isolation

Human EDCs were obtained from atrial appendages donated by patients undergoing clinically-indicated heart surgery after informed consent. All protocols were approved by the University of Ottawa Heart Institute Research Ethics Board (Protocol ID 20150313-01H) and the study was conducted in accordance with the principles of the Declaration of Helsinki. Inclusion of tissue donors were patients requiring cardiac surgery for coronary artery bypass and/or valve surgery. Exclusion criteria included active infection, infectious diseases, pregnancy, and HbA1c greater than 7%.[23,24] EDCs were cultured using standard culture techniques described previously.[21,25,26] Briefly, the atrial appendage tissue was minced to $1mm^3$, washed with cold Hank's Balanced Salt Solution (HBSS, Life Technologies) and enzymatically digested for 30 minutes at 37 degrees Celsius with Collagenase IV (1mg/mL, Life Technologies). Tissue fragments were plated on fibronectin (0.01 mg/mL, Roche)-coated dishes as cardiac explants. EDCs were cultured using serum-free, xenogen-free Nutristem (Sartorius) cell culture media, exposed to 37 degrees Celsius in 5% CO_2 and physiologic oxygen (5%), in a GMP cell manufacturing facility.[27] EDCs spontaneously migrated from the tissue explants after approximately 48 hours and were harvested for direct experimentation every 7 days using mild trypsinization with TrypLE Select (Life Technologies) for 7 minutes at 37 degrees Celsius. Cells were harvested up to 4 times from cardiac biopsies in culture, and manual cells counts were taken using a Neubauer hemocytometer. For cryopreservation, EDCs were stored at -80 degrees Celsius in freezing-medium (Sartorius) and later thawed for downstream applications.

Conditioned media was collected after 48 hours of culture in 1% EV-depleted serum (System Biosciences) and 1% oxygen for centrifugation at 10,000g for 30 minutes and 100,000g

for 3 hours to pellet EVs.[28,29] EV content, size and surface marker expression was analyzed using acetylcholinesterase activity assay (Fluoro-Cet, Systems Biosciences), nanoparticle tracking analysis (NanoSight) and candidate antibody array (Exo-Check, Systems Biosciences) analysis.

3.2 EV miRNA and proteome analysis

The miRNA content within EDC EVs was profiled using multiplex fluorescent oligonucleotide-based miRNA detection (Human v3, Nanostring), as previously described.[28,29] Briefly, miRNA was extracted (miRNeasy, QIAGEN) and quantified (Agilent 2100 Bioanalyzer, Agilent) prior to profiling (Counter Human V3 miRNA Expression Assay). Image quality was evaluated (nSolver) and discarded if the percent field of view and sample binding density exceeded prespecified standards. Background subtraction was performed using the mean of negative controls plus two standard deviations. Counts were normalized using trimmed-mean of M values and differentially expressed miRNA were identified using the generalized linear model likelihood-ratio-test.

EDC EVs were lysed (8 M urea, 100 mM 4-(2-hydroxyethyl)-1-piperazineethanesulfonic acid, 5% glycerol, and 0.5% n-dodecyl β-d-maltoside; Thermo Fischer Scientific), reduced (tris(2-carboxyethyl) phosphine alkylated with iodoacetamide) and digested (trypsin/Lys-C solution, Promega) prior to formic acid treatment, desalination (C18 TopTips, Glygen) and vacuum drying. Protein samples were analyzed using an Orbitrap Fusion mass spectrometer (Thermo Fisher Scientific) coupled to an UltiMate 3000 nanoRSLC (Dionex, Thermo Fisher Scientific) as previously described.[30] Using MaxQuant software, peptides were searched against the human Uniprot FASTA database with a false discovery rate of 1%. Pathway analysis terms were extracted from the Reactome database [31] for network analysis (Cytoscape). Only proteins found in at least 2 biological replicates were considered for analysis.

Flow cytometry was performed on EVs that were individually labelled for CD9 (312106, BioLegend), CD63 (353004, BioLegend), or CD81 (349506, BioLegend) using a CytoFLEX S Beckman Coulter flow cytometer.[32] Light scatter was calibrated using the National Institute of Standards and Technology Traceable Size Standards (Thermo Fischer Scientific) while fluorescence was calibrated using Molecules of Equivalent Soluble Fluorochrome beads (BD Biosciences) for analysis using FCMPASS (v3.07, National Cancer Institute) and FlowJo (V10.7, BD Biosciences).[33] The details of EDC EV characterization have been submitted to the EV-TRACK knowledgebase (EV-TRACK ID: EV210347).[33,34]

3.3 Atrial fibroblast isolation

Primary cultures of rat atrial fibroblasts were isolated from the hearts of middle-aged Sprague-Dawley rats (6 months old, Charles River) using enzymatic digestion (Collagenase Type II, Worthington Biochemical) at 37 degrees Celsius. Cells were cultured in Dulbecco's Modified Eagle High Glucose Medium (DMEM), supplemented with 10% fetal bovine serum (FBS, Thermo Fischer Scientific), 1% l-glutamine (Thermo Fischer Scientific), and 1% penicillin-streptomycin (Thermo Fischer Scientific). Second or third passage fibroblasts were used in all subsequent experiments.

3.4 In vivo study design

To reflect the real-world context and probe for sex-based (biological) differences, the study was performed in both female and male middle-aged rats. Middle-aged Sprague-Dawley rats (6 months old, Charles River) of both sexes underwent induction of sterile pericarditis or sham operation under a protocol approved by the University of Ottawa Animal Care Committee (HI-3137). The detailed protocol was registered a priori within the Open Science Framework (https://osf.io/v9j63/?view_only=0e0ce767cce74bdb8c4fac1b0769a447). A one-way study was

designed to test if intramyocardial injection of EDC EVs at the time of sterile pericarditis induction significantly reduced the incidence of AF during invasive electrophysiological testing (primary outcome). A rat model of sterile pericarditis following talc application was used.[20] To increase the rigour and reproducibility of the study, we studied 6-month-old female and male rats. We assumed that the incidence of AF would be 0.6 after talc treatment and that EV treatment would reduce AF incidence to 0.2. Sex was assumed not to alter the incidence of inducible AF. Based on these assumptions, group sample sizes of 34 rats (17 females + 17 males) would achieve an 83% power to detect superiority over vehicle using a two-sided Mann-Whitney test (probability of a false positive result (alpha error) = 0.05).

3.5 Surgical procedures

Rats were fed rat chow and housed under a 12:12-hour light/dark cycle at 21 degrees Celcius and 50% humidity. All animals had free access to tap water and food. After preoperative buprenorphine (0.03 mg/kg subcutaneous), rats were anesthetized with 3% isoflurane, intubated, and ventilated. The thorax was shaved and sterilized with 2% w/v chlorhexidine gluconate in 70% v/v isopropyl alcohol. Animals were then randomized to sham operation (n=24; 12 females, 12 males), induction of sterile pericarditis with intramyocardial injection of 10^8 atrial EVs (n=35; 18 females, 17 males), or induction of sterile pericarditis with intramyocardial injection of vehicle (n=34; 17 females, 17 males) using a sealed envelope approach. Animals randomized to sterile pericarditis underwent a thoracotomy and the atrial surfaces were dusted with sterile talcum powder (Thermo Fischer Scientific). Animals randomized to a sham procedure underwent a superficial incision that was closed in a manner indistinguishable from thoracotomy animals. Intramyocardial injections were performed using a total volume of 100-µL injected using a Hamilton microsyringe (27-gauge needle) into the left atrial wall at 5 separate injection points.[35]

Injections into the atria were done as superficially as possible. During the injections, a bleb was visible under the epicardial surface, reminiscent of the small blister that forms under the skin when performing an intradermal injection. The needle was then retained at the site of injection for 5 seconds to prevent leakage from the site of injection. Prior to closing the chest, the edges of the pericardium were closely approximated but not sutured together. After surgery, animals were placed in a 30 degrees Celsius incubator with supplemental oxygen and moistened food until they returned to a physiological state. Additional doses of buprenorphine (0.03 mg/kg subcutaneous) were administered 6 and 12 hours postoperatively. A University of Ottawa Animal Care Technician monitored animals twice daily for 2 days after surgery. Investigative staff were blinded to the treatment received and analysis was conducted by individuals blinded to group allocation. Group allocations were kept in a separate password-protected list for unblinding after analysis of the primary study outcome was completed. Ninety-six rats underwent surgery, and all completed the study with no adverse events or protocol deviations (**Supplemental Figure 1**).

Three days after surgery, all rats underwent invasive electrophysiological testing.[35] After intraperitoneal injection of sodium pentobarbital (40 mg/kg), a 1.6F octopolar catheter (Millar) was inserted into the right atrium via the jugular vein for stimulation and recording. The surface electrocardiogram (lead I and II) and intracardiac electrograms (octopolar catheter 1/2, 3/4, 5/6 and 7/8) were continuously simultaneously monitored (AD Instruments). The surface electrocardiogram and intracardiac electrograms were continuously monitored (AD Instruments). The atrioventricular nodal refractory period was determined as the longest S1-S2 interval that failed to conduct to the ventricle using twice-threshold, 2-ms, square-wave pulses after a 10-stimulus drive train (S1, 100-ms cycle length) followed by an S2 decremented in 2-ms intervals. If that failed to induce AF, 10-30 seconds of atrial burst pacing was performed at cycle lengths

that ranged between 20 and 80 ms. AF was defined by rapid and fragmented atrial electrograms without discernible P waves on the surface electrocardiogram and with an irregular ventricular rhythm that lasted for at least 500 ms.[36] AF duration was defined as longest single episode recorded. This data is displayed as the average of the longest episodes of AF for each group of animals. To probe for an effect of EV treatment on the duration of AF, animals that did not experience AF were not included in this average. At the end of the study, rats were sacrificed by exsanguination. Atria were excised and randomly allocated to histological or molecular analysis. All functional evaluations were conducted and analyzed by investigators blinded to the animal's treatment group. A separate cohort of female rats underwent surgery to evaluate the persistence talc and EV effects on fibrosis and inflammation (n=15 per group). Seven days after surgery, animals were sacrificed under pentobarbital anesthesia after displaying absence of withdrawal reflex to toe pinch.

3.6 Histological analysis and quantification of fibrosis

Atria allocated to histology were perfused with saline prior to being excised and fixed with 10% phosphate buffered formalin (Thermo Fischer Scientific) for 72 hours at 4 degrees Celcius. Atria were transferred to 70% ethanol for long-term storage. After embedding within optimal cutting temperature compound, atria were sectioned into 4μm slices, sectioning big surface before being embedded in paraffin. Sections were used for histological analysis of inflammatory infiltrates by staining for hematoxylin and eosin (Sigma), activated T lymphocytes (CD3 (ab16669, Abcam), CD4 (ab237722, Abcam)), macrophage infiltration/polarization (CD68 (ab125212, Abcam), CD163 (ab182422, Abcam)) and neutrophil infiltration (CD11b (ab133357, Abcam)). Briefly, sections were deparaffinized in Xylene (Fisher Scientific) and ethanol prior to an antigen retrieval step performed by boiling slides in either Tris-EDTA-Tween buffer or Citrate

buffer for 1 hour. Slides were blocked with a blocking buffer made up of saline, serum and Triton-X) for 1 hour or overnight prior to application of the primary antibody and 4′, 6-diamidino-2-phenylindole (DAPI, Sigma). All slides were imaged using a Carl Zeiss fluorescent microscope (Axio Observer A1). A list of the secondary antibodies used can be found in **Table 1**. Hematoxylin and eosin staining was quantified using the ImageJ (National Institutes of Health) colour deconvolution plugin.[37,38] Left atrial collagen was quantified based on hydroxyproline content measurement (K555-100, BioVision).[39,40] Atrial fibrosis was confirmed using Masson's Trichrome staining, where fibrosis was defined as the blue area (ThermoFisher).

Name	***Company***	***Catalog Number***
Goat anti-Rabbit IgG Alexa Fluor 488	Invitrogen	A11008
Goat anti-Rabbit IgG Alexa Fluor 594	Invitrogen	A11012

Table 1. List of secondary antibodies used for histology.

3.7 Inflammatory cytokines

Atrial tissue was minced and homogenized using a tissue homogenizer (TissueRuptor, Qiagen) according to the manufacturer protocol. Inflammatory cytokines and chemokines were measured using a multiplex Luminex-based assay (LXSARM, R&D Systems). Each sample was run in duplicate in a 96-well plate. Interleukin 1 beta (IL1β), IL2, IL18, and tumour necrosis factor alpha (TNFα) were measured using a MAGPIX system (C4447b). Acquired mean fluorescence data were analyzed and calculated by the xPONENT software. IL6 (ERA32RB, Invitrogen), transforming growth factor beta 1 (TGFβ1, ab119558, Abcam), platelet-derived growth factor-AB (PDGF-AB, ab213906, Abcam) and monocyte chemoattractant protein 1 (MCP1, ab100778, Abcam) were quantified using commercially available enzyme-linked immunosorbent assays (ELISA) according to the manufacturer protocol.

3.8 Fibroblast proliferation

The POAF cellular context was modeled by exposing normal rat atrial fibroblasts to IL6 or TGFβ1 to recapitulate the inflammatory in vivo environment.[41] Proliferation of atrial fibroblasts at baseline and after treatment with IL6, TGFβ1, and/or EDC EVs was evaluated by staining for the nuclear incorporation of the thymidine analogue 5-ethynyl-2´-deoxyuridine (EdU, 17-10525, Millipore) and 4′,6-diamidino-2-phenylindole (DAPI, Sigma). Manual cell counts were performed to confirm the findings. Population doubling time was measured with a colorimetric assay (Dojindo). Cell-cycle distribution was evaluated via flow cytometry according to the manufacturer's instructions (4500-0220, Guava). Briefly, fibroblasts were cultured for 24 hours with 10^8 atrial EVs, IL6, TGFβ1, a G1 cell arrest control (aphidicolin (APC, Sigma)) or vehicle. Flow cytometry was performed to quantify populations within G0/G1, S, and G2/M phases of the cell cycle for each treatment (Guava, Millipore Sigma). To further explore the effect of EDC EVs on atrial fibroblasts, commercially available ELISAs were performed to look at the molecular regulators of cell cycle progression. Atrial fibroblasts were lysed according to the manufacturer's instructions and ELISAs were performed for Cyclin A2 (MBS7211946, MyBioSource), B1 (MBS9328611, MyBioSource), D (MBS721009, MyBioSource) and E (MBS1600300, MyBioSource).

3.9 Statistical analyses

All statistical tests used and graphical depictions of data (means and error bars, or box and whisker plots) are defined within the figure legends for the respective data panels. All data are presented as mean ± standard error of the mean. To determine if differences existed between groups, data were first analyzed by one-way ANOVA (SPSS v20.0.0); if among-group differences existed, Bonferroni's corrected t-test was used to determine the statistical significance of

intergroup differences. In all cases, variances were assumed to be equal and normality was confirmed prior to post-hoc testing. Differences in categorical measures were analyzed using a Chi Square test. A final value of $P \leq 0.05$ was considered significant for all analyses.

4.0 RESULTS

4.1 Human atrial EVs contain anti-fibrotic/anti-inflammatory transcripts and proteins

Human EDCs were cultured in a clinical cell manufacturing facility from atrial appendage biopsies using serum-free xenogen-free culture conditions. EVs were isolated from conditioned media after 48 hours in 1% oxygen, basal media conditions.[21,29] In keeping with accepted definitions, EDC EVs represented a polydisperse population of particles that ranged in diameter from 95 to 170 nm (132±7 nm). These microparticles contained transmembrane (CD63, CD81, FLOT1, ICAM1, EpCam) and cytosolic (ALIX, ANXA5 and TSG101) markers indicative of EV identity[42] while lacking evidence for cellular contaminants (GM130; **Figure 1A**). Flow cytometry demonstrated significant enrichment of micro-particles with the prototypical EV markers CD9, CD63, CD81 **(Figure 1B and Supplemental Figure 2**). Interestingly, there were fewer particles that expressed CD81 (~2-fold less, $p<0.05$ vs. CD9 or CD63) while smaller particles were more apt to express CD63 ($p<0.05$ vs. CD9 or CD81). Acetylcholinesterase activity was also present and correlated with nanoparticle particle tracking content (**Figure 1C**). These results confirm the presence of a functional extracellular membrane-bound protein associated with EVs and provide a rapid means of confirming EV concentration.

The cargo within EDC EVs was enriched with 83 miRNA transcripts associated with reducing inflammation, stimulating angiogenesis, and suppressing fibrosis **(Figure 1D and Supplemental Figure 3**). Interestingly, the most abundant miRNAs (1000+ counts) were associated with altered cell division/proliferation (let-7a, miR23a and miR-199a) and fibrosis (let-7a and miR-199a). Although EDC EVs contained miR-21, a transcript known to promote fibrosis and AF susceptibility[35], they lacked all other known pathological transcripts (miR-1,[43] miR-133,[44] miR-328[45] and miR-590[46]) and included miRNAs associated with reduced fibrotic atrial

remodeling (miR-26 and miR-29[47,48]). Within the 811 proteins identified within EDC EVs (**Figure 2**), the proteome was enriched with 196 proteins associated with reducing inflammation (Wilcoxon rank sum test $p<0.003$), which directly influenced both chemotaxis (i.e., annexin A1 and annexin-5)[49-53] and macrophage function (i.e., galectin-1, hemopexin and thioredoxin)[54-58]. Among the 28 proteins implicated in reducing fibrosis, decorin (a TGFβ1 inhibitor) and matrix metalloproteinase 2 were highly expressed.[59-62] Enrichment mapping of the EV proteome predicted important roles in regulation of cell cycle, inflammation and cellular signaling.

Taken together, this data supports the notion that EDCs produce a defined EV product containing an anti-fibrotic, anti-inflammatory cargo with the potential to alter the fundamental drivers of POAF.

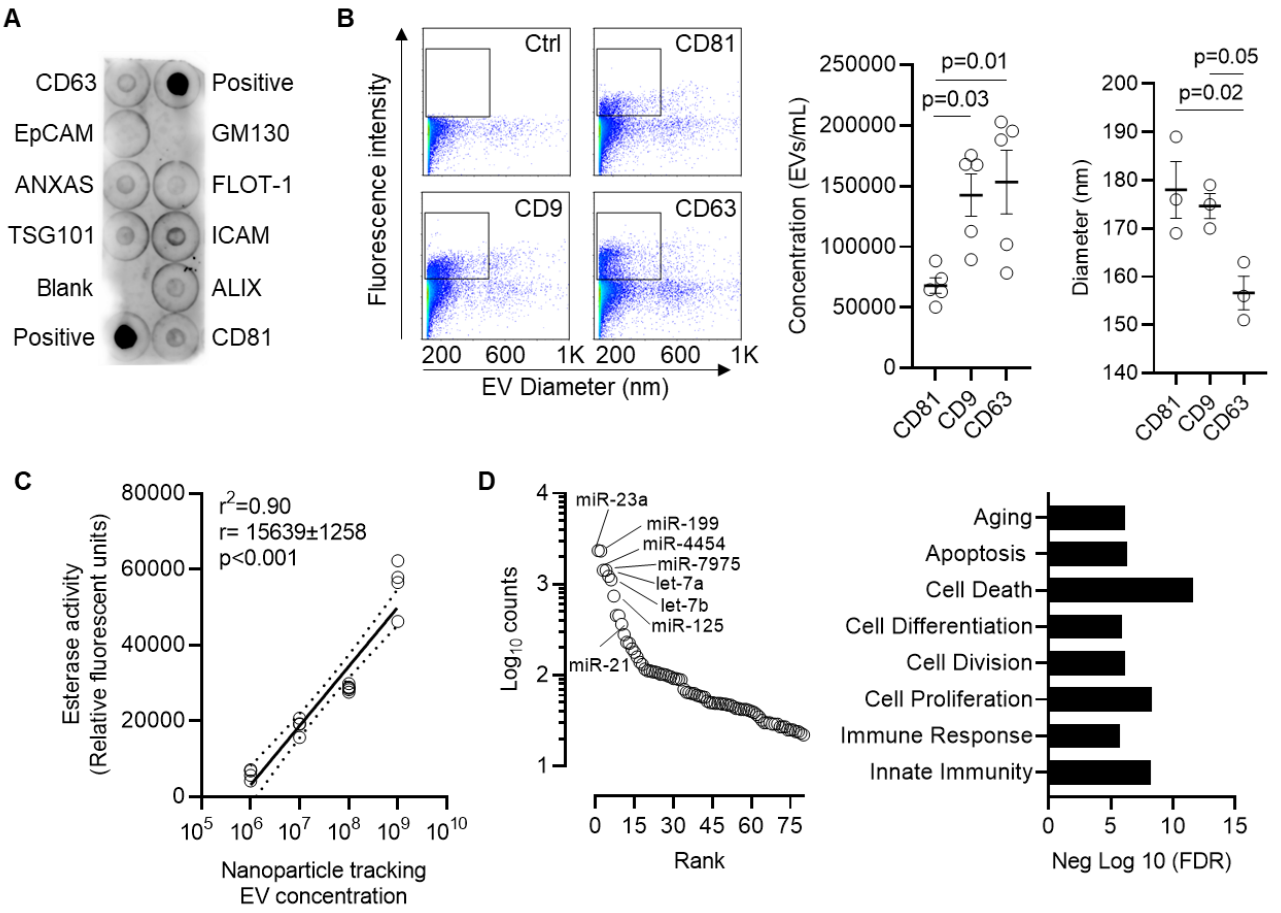

Figure 1. Characterization of extracellular vesicles produced by human atrial explant-derived cells cultured under serum-free xenogen-free culture conditions within a clinical cell manufacturing facility. **(A)** Proteomic array demonstrating presence of markers indicative of EV identity while lacking cellular contaminants. **(B)** Flow cytometry demonstrating the relationship between EV size and surface marker expression (n=3 biological replicates). One-way ANOVA with individual-mean comparisons by Bonferroni's multiple two-tailed comparisons test. **(C)** Simple linear regression of the relationship between EV concentration and acetylcholinesterase activity (n=5 biological replicates). Data is plotted showing the 95% confidence bands of the best fit line. **(D)** Relative abundance of microRNA transcripts within EDC EVs (n=3 biological replicates). EV, extracellular vesicles; FDR, false discovery rate; miR, microRNA.

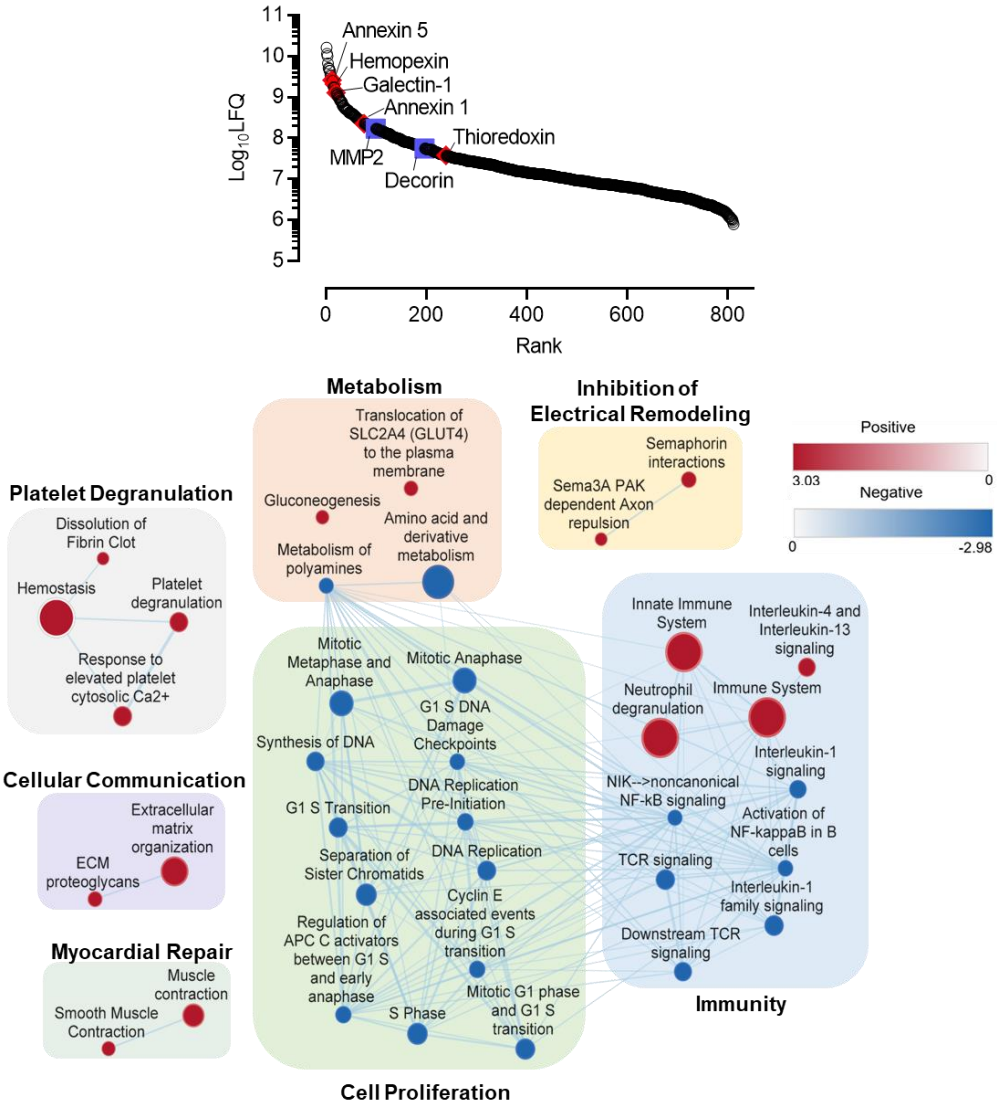

Figure 2. Human atrial explant-derived cells cultured under serum-free xenogen-free culture conditions within a clinical cell manufacturing facility produce extracellular vesicles that contain anti-fibrotic/anti-inflammatory proteins. Relative abundance of proteins within EDC EVs (n=3 biological replicates). Enrichment map of the EDV EV proteome demonstrating the relationship between biological pathways that are expressed more than would be expected by chance. Pathways are represented by circles (nodes) connected with lines (edges) according to the number of shared proteins. Node size reflects the number of proteins participating in each pathway. The number of proteins shared by connected pathway nodes determines the thickness of edges.

Upregulated pathways are colored red while downregulated pathways are in blue. The color of the concentric circles around each node represents the level of enrichment based on the enrichment score scale provided. Groupings of pathways are labeled by common activities or functions. ECM, extracellular matrix; LFQ, label-free quantification; MMP2, matrix metalloprotein 2.

4.2 Intramyocardial injection of human EVs reduce inflammation, fibrosis and fibrillation

The antiarrhythmic potential of EVs against POAF was explored using a rat model of sterile pericarditis,[20] whereby animals underwent open-chest surgery before randomization to epicardial application of talc or no talc (**Figure 3A**). Immediately after epicardial application of talc, animals were randomized again to trans epicardial intra-myocardial injection of EVs or vehicle (saline; **Figure 3A**) into the atrial tissue. As outlined in **Supplemental Figure 1**, all animals survived the initial surgery, while 3 animals died because of anesthetic overdose prior to the second procedure (all proving to be vehicle-treated). Treatment with EVs reduced the probability of inducing AF 3 days after open-chest surgery by 40% ($p<0.01$ vs. vehicle alone, **Figures 3B and 3C**). Recipient sex did not alter this effect. In animals that experienced AF, neither EV treatment or recipient sex significantly altered AF duration (**Figure 3D**); although the lack of statistical significance may be due to the very low number of sham and EV treated animals (4 and 9 respectively) that experienced AF and the non-parametric distribution of AF duration. Pericarditis, EV treatment and recipient sex had no effect on electrocardiographic or electrophysiological measures of cardiac function (**Supplemental Table 1**). As shown in **Figure 3E**, EV treatment attenuated atrial fibrosis (45±19% reduction in hydroxyproline content, $p=0.01$, vs. vehicle alone; 28±19% reduction in Masson's Trichrome scar content, $p=0.01$ vs. vehicle alone;

Supplemental Figure 4) and enlargement (41±15% reduction in atrial/body weight, p=0.01, vs. vehicle alone).

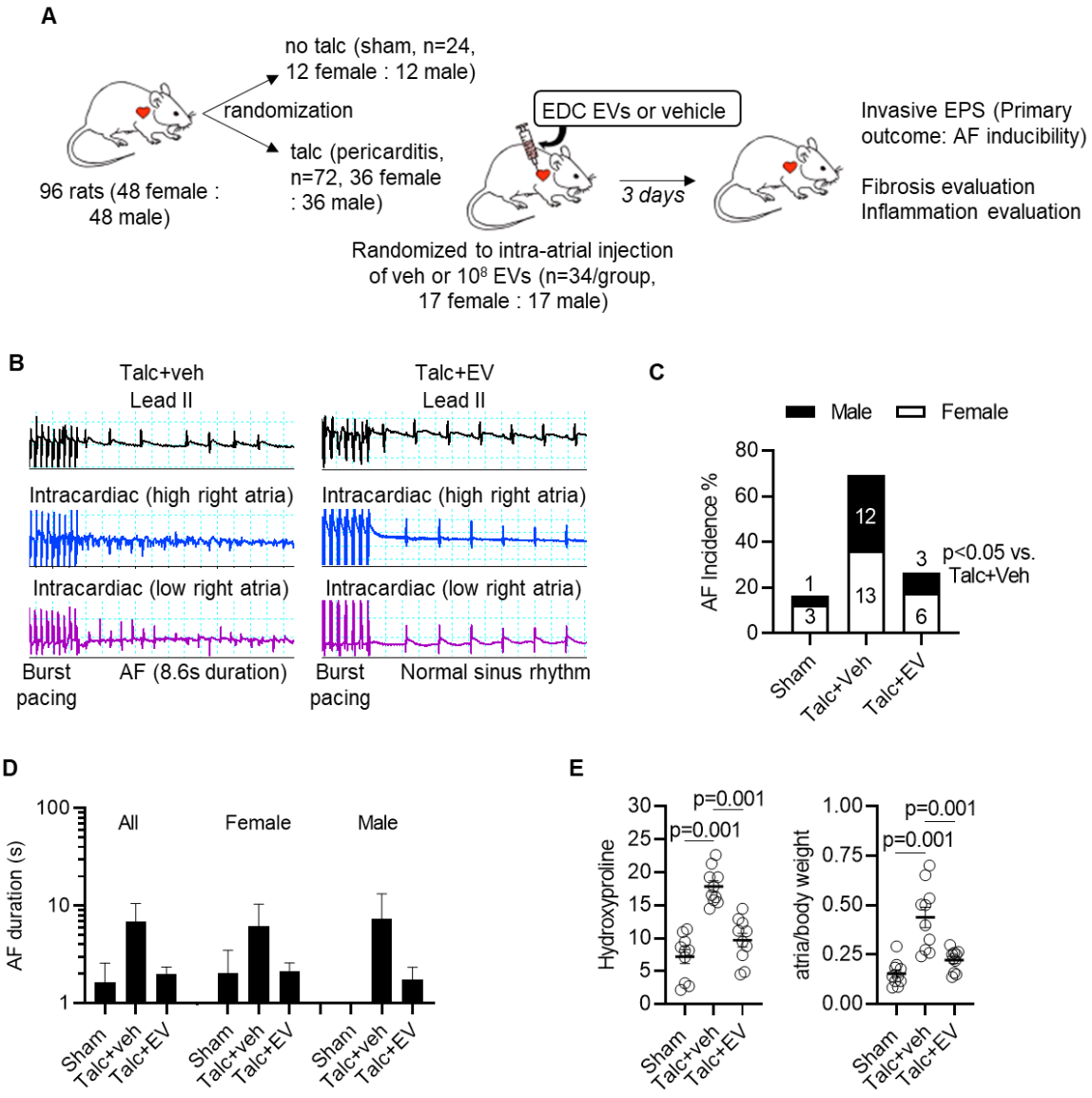

Figure 3. Human atrial extracellular vesicle effects on post-operative AF and atrial structure. **(A)** Study schematic demonstrating the study design, numbers of animals included, group allocations and outcomes measured. One additional female rat was inadvertently randomized to receive extracellular vesicles (EVs) and was included in the final analysis (n=18 females talc+EV group only). **(B)** Two representative tracings showing the effect of EV treatment on talc-treated

animals after burst pacing. **(C)** Effect of EV treatment on the probability of inducing AF after burst pacing. Superimposed numbers indicate the absolute number of female (lower grey bar + number) or male (upper black bar + number) animals that went into AF. Logistic regression using a generalized linear model with binomial probability distribution and the logit link function was performed. **(D)** Effect of EV treatment on the mean duration of AF episodes (n=2-25). **(E)** Effect of EV treatment on hydroxyproline content (n=10), Masson's Trichrome fibrosis (n=6-8) and structure (n=10). One-way ANOVA with individual-mean comparisons by Bonferroni's multiple two-tailed comparisons test. AF, Atrial fibrillation; EDCs, explant-derived cells; EPS, electrophysiological study; EV, extracellular vesicles; veh, vehicle.

4.3 EVs prevent inflammation and polarize atrial macrophages to a pro-healing phenotype

Open chest surgery results in loss of the pericardial mesothelial cells which provokes inflammatory infiltration and a fibrinous reaction.[63] The influence of human EVs on inflammation was first evaluated using atrial histology of EV treated rats. As shown in **Figure 4A**, sterile pericarditis markedly increased the inflammatory infiltrate detected in atrial sections (6±2-fold increase, $p<0.001$ vs. baseline). EV injection attenuated the inflammatory effect of talc as the inflammatory infiltrate was halved (47±23% less; $p<0.001$ vs. vehicle treatment). This decrease reflected the reduction in pro-inflammatory cytokines found in treated atria (**Figure 4B**). Sterile pericarditis alone resulted in prototypical increases of the pro-inflammatory cytokines IL1β, IL2, IL6, IL18, MCP1, TGFβ1, PDGF-AB and TNFα. Intramyocardial injection of EVs prevented the rise in a number of these cytokines (IL2, IL6, PDGF-AB, TGFβ1 and TNFα) while attenuating the observed increase in others (IL1β, IL18, MCP1).

To explore the mechanism underlying these observed changes, we profiled the inflammatory infiltrates found within the atria 3 days after surgery. As shown in **Figure 5A and Supplemental Figure 5**, sterile pericarditis increased the number of neutrophils (CD11b), cytotoxic T cells (CD3) and T helper cells (CD4) found in the atria. EV treatment significantly decreased the recruitment of all 3 cell types to near-baseline values. Sterile pericarditis also increased the atrial content of pro-inflammatory M1 macrophages expressing the surface marker CD68 by 4.5±1.1 fold from sham ($p<0.01$, **Figure 5B**). Although M1 macrophages were also increased in EV treated rats, this increase was significantly attenuated to 1.6±0.5 fold ($p=0.01$ vs sham). Interestingly, sterile pericarditis also increased the number of pro-healing anti-inflammatory M2 macrophages (CD163-expressing) by 1.8±0.5 fold from sham ($p<0.01$). EV treatment markedly increased atrial content of CD163 macrophages (4.3±1.0 fold greater, $p<0.01$ vs. sham. $p<0.01$ vs. vehicle-treated) suggesting that EV treatment promoted macrophage polarization towards an anti-inflammatory phenotype that may help to attenuate the inflammatory response.

The long-term consequences of sterile inflammation induced by talc was evaluated in a series of animals sacrificed 7 days after surgery (**Supplemental Figure 6A**). Pericarditis resulted in persistent chamber enlargement and increases in measures of fibrosis (hydroxyproline and Masson's Trichrome; **Supplemental Figure 6B and 6C**). The changes mirrored persistent increases in inflammatory infiltrates (**Supplemental Figure 7A**) and inflammatory cytokines (**Supplemental Figure 7B**). Akin to the effects seen 3 days after surgery, EVs attenuated the effects of pericarditis on fibrosis, chamber enlargement, inflammatory infiltration, and inflammatory cytokine abundance (59 ± 4 vs. 39 ± 3 or 22 ±5% viable myocardium within ischemic risk area, $p<0.05$ vs. suspended EDCs or vehicle, respectively).

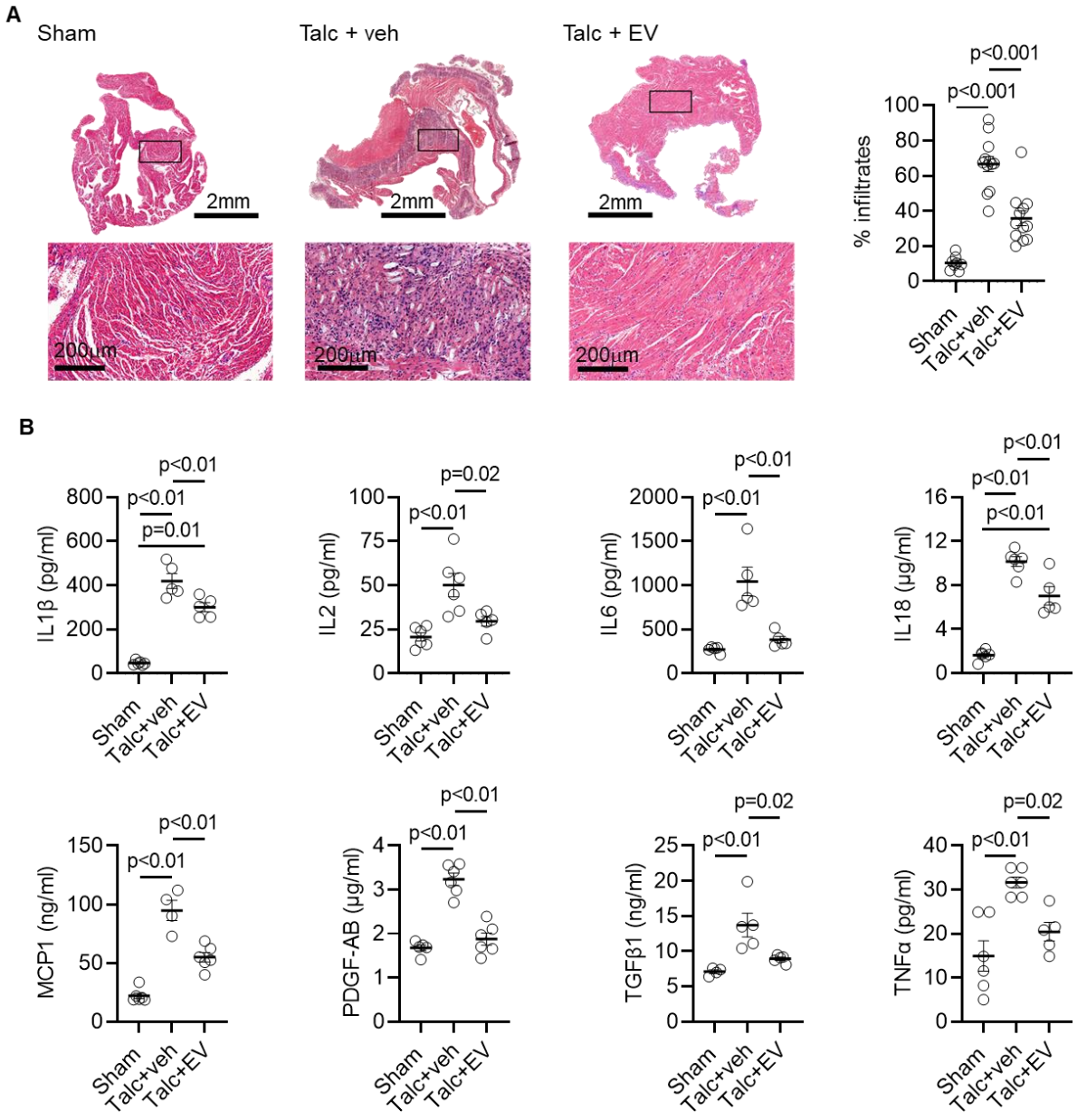

Figure 4. Effect of human atrial extracellular vesicles on inflammation. (**A**) Representative images of atrial tissue sections after hematoxylin and eosin staining showing the effect of talc and extracellular vesicles (EVs) on inflammatory cell infiltration. Quantitative analysis showing the effect of talc and EVs on inflammatory cell infiltration (n=8-12 biological replicates). (**B**) Effect of talc and EVs on interleukin 1 beta (IL1β), IL2, IL6, IL18, monocyte chemoattractant protein 1

(MCP1), platelet-derived growth factor AB (PDGF-AB), transforming growth factor beta 1 (TGFβ1) and tumor necrosis factor alpha (TNFα) expression (n=4-6 biological replicates). One-way ANOVA with individual-mean comparisons by Bonferroni's multiple two-tailed comparisons test. Scale bar, 2 mm or 200 μm, as indicated.

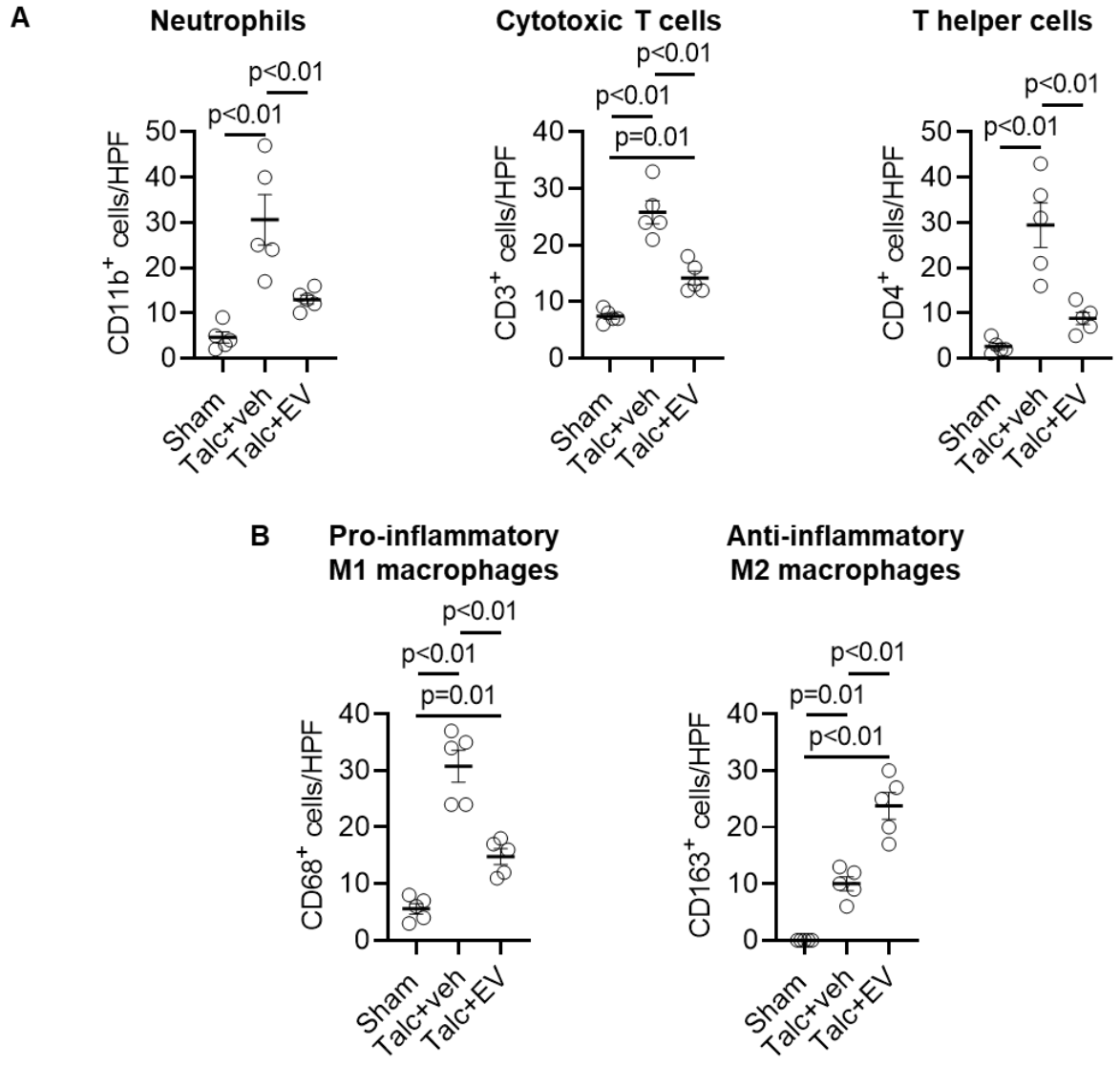

Figure 5. Effect of human atrial extracellular vesicles on inflammatory cell infiltration. (**A**) Effect of explant-derived cell (EDC) extracellular vesicles (EVs) on the number of neutrophils (CD11b), cytotoxic T cells (CD3) and T helper cells (CD4) found within treated atria (n=5

biological replicates, 6 random fields per biological replicate). (**B**) Effect of talc and EVs on the atrial content of pro-inflammatory M1 macrophages (CD68) and anti-inflammatory M2 macrophages (CD163, n=5 biological replicates, 6 random fields per biological replicate). One-way ANOVA with individual-mean comparisons by Bonferroni's multiple two-tailed comparisons test.

4.4 EVs directly prevent the activation of atrial fibroblasts

Fibroblasts comprise almost 75% of the cells within the heart.[64] When fibroblasts are activated by profibrotic stimuli, they proliferate and differentiate into myofibroblasts, which reconfigure the extracellular matrix and can have adverse effects on atrial structure and electrophysiological function. Given that interfering with atrial fibroblast proliferation reduces fibrosis and AF burden, we explored the influence of EVs on atrial fibroblast proliferation. POAF was modeled by exposing normal rat atrial fibroblasts to interleukin-6 (IL6) or transforming growth factor beta 1 (TGFβ1)[41]. As shown in **Figure 6A and Supplemental Figure 8**, IL6 and TGFβ1 increased fibroblast proliferation as evidenced by increases in manual cell counts and EdU incorporation. Application of EVs at the time of IL6/TGFβ1 exposure restored fibroblast proliferation back to baseline.

Flow cytometry was used to profile the effects of EVs on cell-cycle kinetics (**Figure 6B**). Fibroblasts grown in high serum conditions demonstrated progression through the cell cycle (G0/G1, S, and G2/M phases). Aphidicolin (APC) promoted degradation of cell-cycle proteins and cells accumulated in the G0/G1 phase. IL6 and TGFβ1 reduced the proportion of fibroblasts within G0/G1 phase by 15±4% ($p=0.004$ vs. baseline) and 15±8% ($p=0.005$ vs. baseline) while increasing the proportion of cells in the proliferative S+G2M phases by 24±7% ($p=0.01$ vs. baseline) and

24±12% (p=0.01 vs. baseline), respectively. Co-administration of EVs abrogated the effects of each cytokine on the proportional changes in G0/G1 and S+G2M fibroblasts (p=ns vs. baseline). Fibroblast cultures were then interrogated to identify which cyclins within the regulatory machinery underlying cell cycle progression were modified by EV treatment. As shown in **Figure 6C**, treatment with IL6 or TGFβ1 increased the content of cyclins A2, B1 and E while decreasing the content of cyclin D well below baseline values. Co-administration with EDC EVs attenuated these effects, with cyclins levels often normalizing after treatment. Interestingly, EV treatment decreased expression of cyclin B1 below baseline in a manner consistent with the observed effects on proliferation.

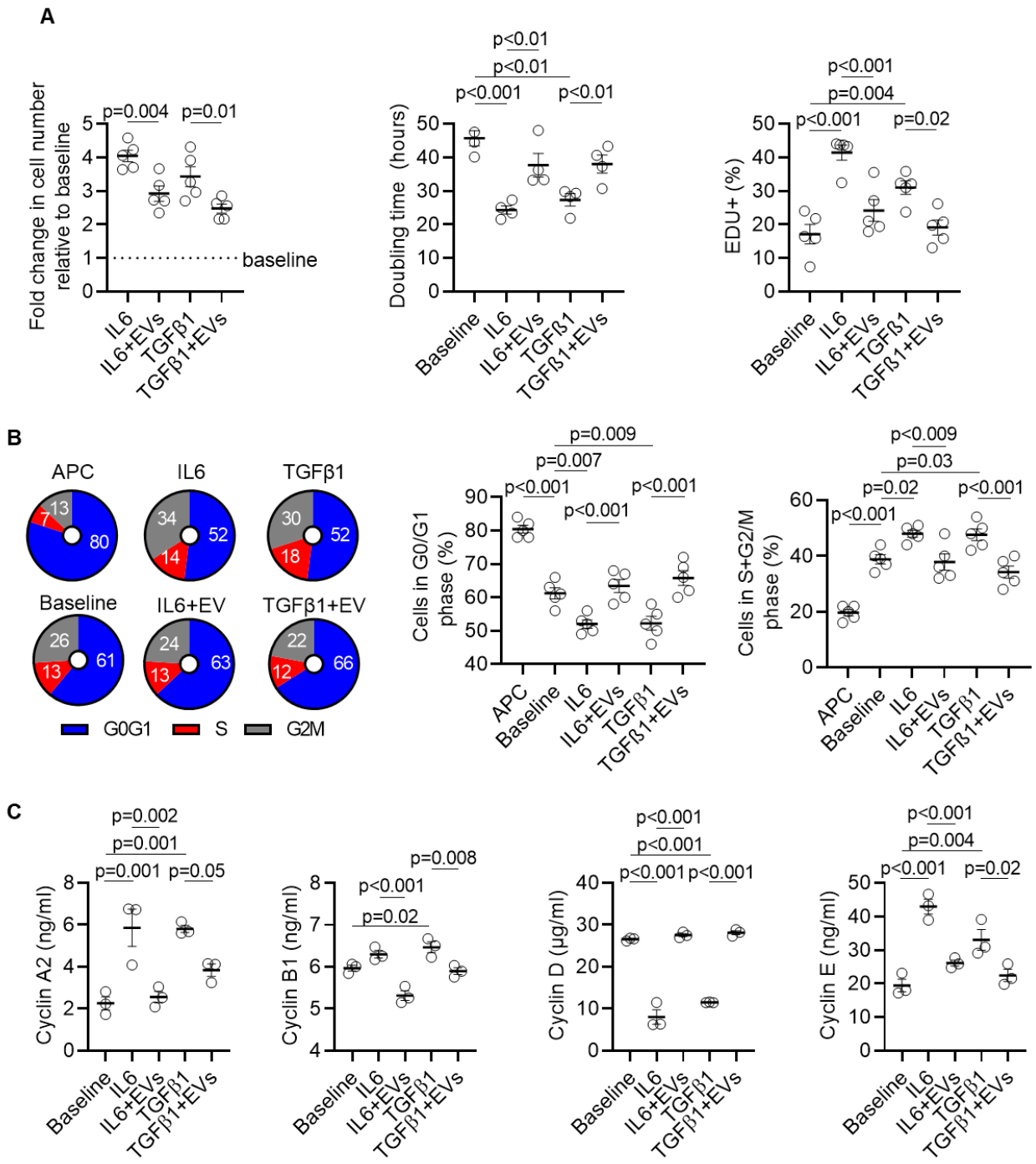

Figure 6. Effect of human atrial extracellular vesicles on atrial fibroblast proliferation. (A) Effect of explant-derived cell (EDC) EVs on the relative cell number, population doubling time and nuclear incorporation of the thymidine analogue 5-ethynyl-2´-deoxyuridine (EdU) within atrial fibroblasts at baseline and after treatment with interleukin 6 (IL6), transforming growth

factor beta 1 (TGFβ1), and/or EDC EVs (n=5 biological replicates). Baseline indicates normal high serum conditions. (**B**) Cell cycle analysis showing the effect of anaphase-promoting complex (APC), IL6, TGFβ1 and/or EDC EVs on the proportion of atrial fibroblasts in the G0/G1 or S and G2/M phases of the cell cycle (n=5 biological replicates). Baseline indicates normal high serum conditions. (**C**) Effect of IL6, TGFβ1 and/or EDC EVs on proteomic expression of cyclins that control progression of atrial fibroblasts through the cell cycle (n=3 biological replicates). Baseline indicates normal high serum conditions One-way ANOVA with individual-mean comparisons by Bonferroni's multiple two-tailed comparisons test.

5.0 DISCUSSION

Conventional therapies for POAF reflect approaches to attain and maintain normal rhythm while preventing rate-related complications and systemic embolization.[7] Despite these measures, a single occurrence of POAF often extends hospital length of stay and increases costs.[4,5] To date, only prophylactic beta-blockers, which target the autonomic alterations associated with surgery, are routinely recommended to reduce the incidence of POAF.[9] Given that the onset of POAF typically occurs 1 to 3 days after surgery, any therapy needs to be administered before the injury, influence function during this critical 1-3 day recovery period and not have adverse effects on post-operative recovery. In this study, we explored the concept that an intra-myocardial dose of EVs injected into the atria would prevent inducible AF after open-chest surgery without a need for interventional procedures or systemic drugs. Atrial inflammation, one of the key drivers of POAF, was attenuated. In a manner consistent with the known anti-fibrotic effects of EVs on post-infarct ventricular remodeling,[21,25,26,28,29,37], EVs rendered atrial fibroblasts inert to the pro-fibrotic effects of inflammation. The importance of these effects was manifested by a great reduction in AF inducibility 3 days after open chest surgery.

The pathogenesis of POAF revolves around the interaction between preoperative, perioperative, and postoperative factors.[65] Patients who are referred for surgery often present with a pre-existing, adversely remodeled, atrial substrate that reflects advanced age and other medical comorbidities. Surgery itself exposes patients to peri-operative risks (such as anesthetics, atriotomy incisions, cardiopulmonary bypass, and electrolyte abnormalities) that further reduce the threshold for AF. Several days after surgery, autonomic nervous system activation, inflammation, oxidative stress, and atrial stretch combine to increase atrial vulnerability so that ectopic beats can initiate POAF. In this report, we tested the idea that a single intra-atrial injection

of EVs can attenuate postoperative factors that increase substrate vulnerability to AF, in particular inflammation and the pro-fibrillatory transformation of atrial fibroblasts. In support of this mechanistic link, we demonstrated that EVs reduced neutrophil infiltration, proinflammatory macrophage polarization and inflammatory cytokine production. Conceptually, EVs must pre-condition resident atrial cells to limit inflammatory signaling. This mechanism is consistent with ventricular remodeling studies which show that EVs from heart-derived cells change the polarization state of resident and infiltrating macrophages,[16,66] and with studies showing a role for atrial cardiomyocyte inflammatory signaling in POAF.[67] Interestingly, a single dose of EVs also reduced atrial fibrosis, a component of the structural remodeling known to ensue after surgery.[68] This in vivo effect may in part be attributable to inhibition of pro-inflammatory cytokines produced by resident cells but in vitro profiling suggests that EV treatment renders atrial fibroblasts anti-fibrotic and resistant to pro-inflammatory stimuli.[18] Thus, EV treatment leverages several mechanisms to reduce substrate vulnerability below the threshold at which triggers do not initiate POAF.

These results contrast with other preclinical approaches to POAF in several ways. Firstly, our study design fulfills many of the SYRCLE criteria used to exclude bias[69] and many of the CAMARADES checkpoints used to evaluate study quality.[70] We also chose to examine the clinically meaningful "incidence of inducible AF" for our primary outcome rather than total duration of AF. Unlike most pre-clinical studies to date,[12,13] the scalable biological product used in this study was cultured to GMP cell manufacturing standards using sourced xenogen-free materials which makes clinical translation relatively straightforward. To maximize benefit to the treated substrate, we evaluated a biological product that simultaneously targets many different mechanistic pathways known to contribute to POAF vulnerability rather than focus on a single

mechanism that may leave a host of other fundamental changes initiating and maintaining AF unaddressed.[47,71-76] In contrast to a drug or a single miRNA transcript, EVs are manufactured by producer cell lines. As such, they provide a platform amenable to engineering refinements. Although EDC EVs possess many miRNA transcripts known to reduce fibrotic atrial remodeling (miR-26 and miR-29)[47,48], they also contain the pro-arrhythmic transcript miR-21.[35] Thus, relatively simple engineering of producer cell lines to knock down pathological transcripts within EVs has the potential to further enhance the anti-arrhythmic potency, a concept requiring further experimental assessment. Finally, systemic therapies often may have unwanted off-target effects such as impaired wound healing, infection, hyperglycemia, gastritis, proarrhythmia or myelosuppression. The demonstration that a single injection of EVs directly into the target tissue provides marked lasting benefits is interesting because such a local approach is unlikely to be limited by off-target adverse effects in remote tissues.

Despite these promising features and results, this study has several potential limitations that need to be acknowledged. Although rodents provide a cost-effective means of testing new therapies, their repolarizing ion-channel profile and basal heart rates differ from those of humans. Rodent hearts are also inherently much smaller and do not generally exhibit spontaneous AF, requiring AF induction to obtain indices of the AF substrate. Our findings rationalize future work using large animal models that better reflect human electrophysiology and provide the opportunity for realistic clinical scaling. We also recognize that the extent to which EVs may act upon the preoperative components of the vulnerable substrate for AF is speculative and not the focus of this study, as none of the treated animals had a pre-existing atrial cardiomyopathy. However, this approach has merit, as similar studies looking at delayed administration of EVs after myocardial ischemia[17,37] suggest that treatment has the potential to promote salutary atrial remodeling which

may reduce vulnerability to AF. Similarly, the extent to which EV treatment alters the substrate-effects of cardiac incision, open-heart surgery and cardiopulmonary bypass-related systemic inflammation was not examined in this model, as none of the animals had surgical cardiac lesions or underwent cardiopulmonary bypass.

In summary, our study indicates that a single dose of EVs delivered at the time of open-chest surgery directly into the affected area (i.e., the atria) before the disease starts has the potential to target multiple pathways that result in AF. Our work has shown that scaling using serum-free, xenogen-free techniques is feasible and will provide a cost-effective product for clinical use. This approach merits future attention as assessment in patients would be relatively straightforward, the clinical problem addressed is quite significant and clinical event rates are high.

6.0 CONCLUSION

Intramyocardial injection of EVs at the time of open chest surgery provides a facile acellular strategy to prevent POAF by reducing inflammation and fibrosis. This of great importance because 500,000 patients/year undergo open chest surgery and 50% of them will experience POAF. Currently, there are little options for these patients as post-surgical guidelines render conventional treatments contra-indicated or even ineffective after surgery. This study indicates that a single intramyocardial injection of EVs directly into the atria at the time of open chest surgery by surgeons may target the multiple pathways needed to prevent atrial fibrillation and reduce adverse clinical outcomes needed for these patients.

7.0 SUPPLEMENTAL FIGURES & TABLES

7.1 In vivo study conduct and group sizes

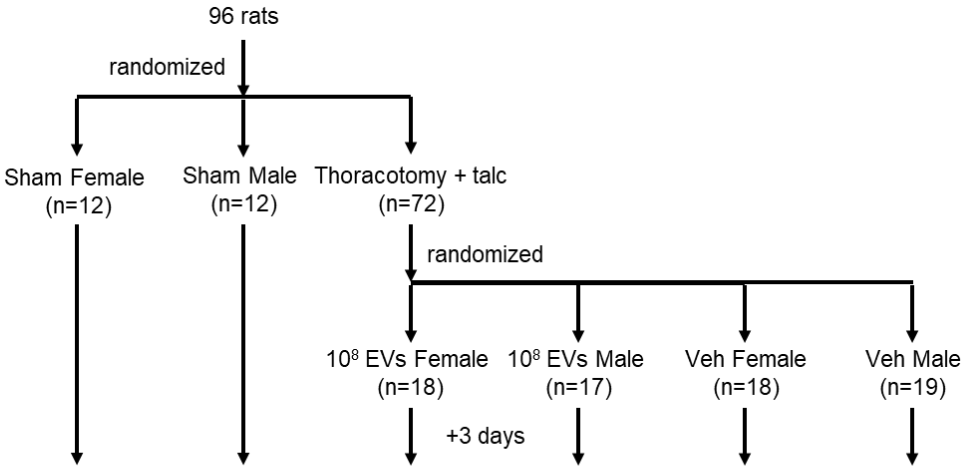

Adverse outcomes						
Died after initial surgery	0	0	0	0	0	0
Died after second surgery	0	0	0	0	1	2
Primary outcome						
In vivo EPS:	12	12	18	17	17	17
Secondary outcomes						
Histological analysis:	8		12		12	
Hydroxyproline analysis:	10		10		10	
Inflammatory cytokines:	6		6		6	

Supplement Figure S1. **In vivo study conduct and group sizes.** We assumed the incidence of atrial fibrillation (AF) would be 0.6 after talc treatment and that extracellular vesicle (EV) treatment would reduce AF incidence to 0.2. Sex was assumed not to alter the incidence of inducible AF. Based on these assumptions, group sample sizes of 34 rats (17 females + 17 males) would achieve an 83% power to detect superiority using a two-sided Mann-Whitney test (probability of a false positive result (alpha error) = 0.05). Animals that died because of anesthetic

overdose prior to the second procedure were not included in the analysis. An allocation error resulted in 1 additional female rat receiving EVs. To avoid compromising the data, the animal was included in the analysis. Given that recipient sex did not influence occurrence of the primary outcome (i.e., AF inducibility), secondary outcomes (e.g., histology, fibrosis, cytokines, etc.) were not analyzed separately for recipient sex. EPS, electrophysiological study, EV, extracellular vesicle, veh, vehicle.

7.2 Flow cytometry of extracellular vesicles

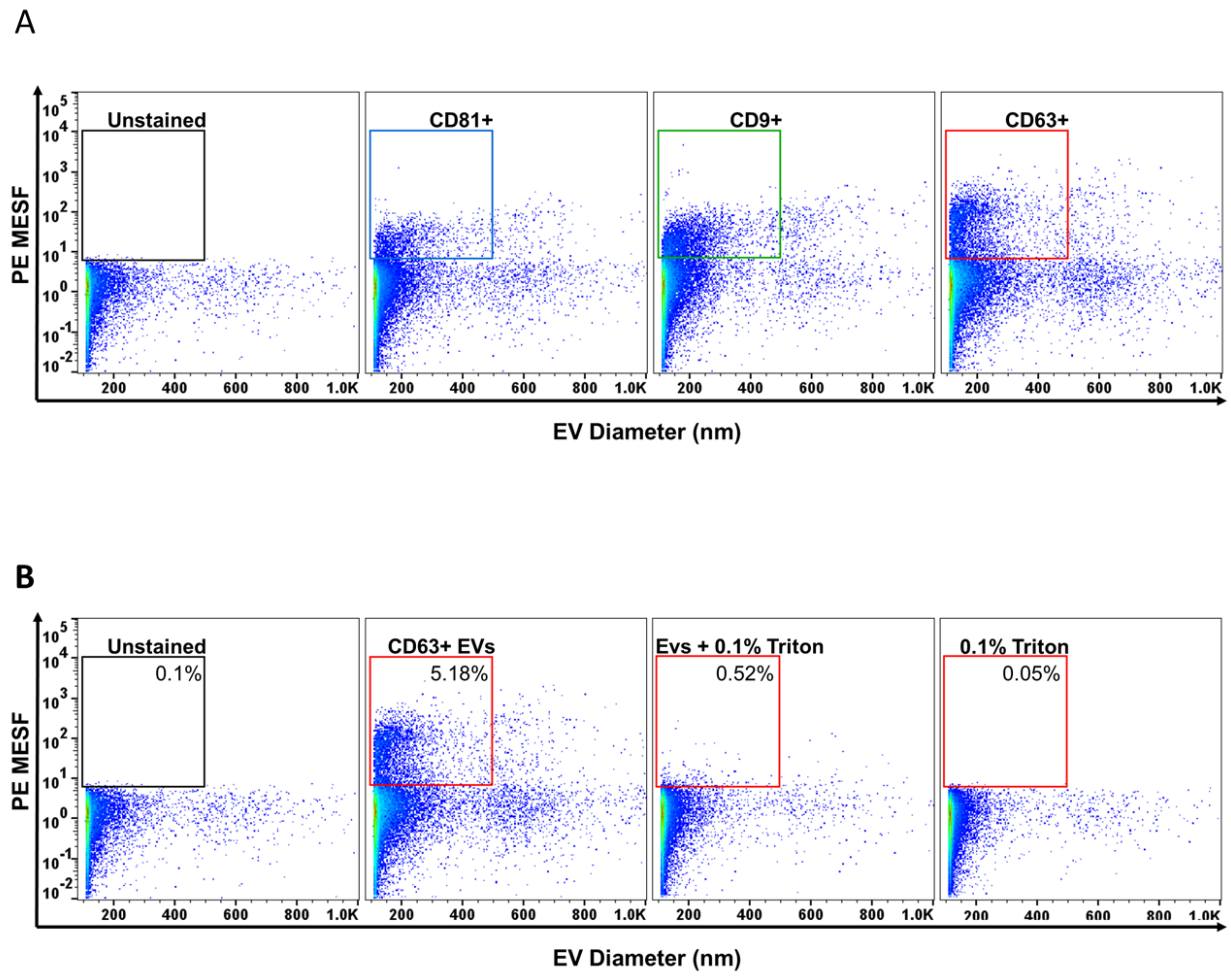

Supplement Figure S2. **Flow cytometry of extracellular vesicles.** (**A**) Representative images showing the relationship between extracellular vesicle (EV) diameter and surface marker expression. EVs within a range of 100 – 500 nm in diameter are gated. Fluorescence intensity is quantified using standard units known as Molecules of Equivalent Soluble Fluorochrome (MESF). (**B**) Representative image of flow cytometry demonstrating EV depletion after solubilization. The addition of 0.1% Triton X-100 solubilizes CD63 stained EVs. Number inside the gates represent percentage of gated population within all particles detected. PE MSEF, Phycoerythrin Molecules of Equivalent Soluble Fluorochrome.

7.3 MicroRNA transcript expression within explant-derived cell extracellular vesicles

	Average counts
hsa-miR-23a-3p	2355
hsa-miR-199a-3p+hsa-miR-199b-3p	2326
hsa-miR-4454+hsa-miR-7975	1426
hsa-let-7a-5p	1221
hsa-let-7b-5p	1122
hsa-miR-125b-5p	743
hsa-miR-100-5p	453
hsa-miR-29b-3p	450
hsa-miR-21-5p	362
hsa-miR-191-5p	279
hsa-miR-199b-5p	230
hsa-miR-29a-3p	224
hsa-miR-22-3p	195
hsa-let-7i-5p	178
hsa-miR-181a-5p	159
hsa-miR-25-3p	139
hsa-miR-127-3p	131
hsa-let-7g-5p	117
hsa-miR-15b-5p	112
hsa-miR-320e	112
hsa-miR-221-3p	109
hsa-let-7d-5p	108
hsa-miR-16-5p	106
hsa-miR-424-5p	102
hsa-miR-3180	102
hsa-miR-374a-5p	101
hsa-miR-15a-5p	98
hsa-miR-130a-3p	96
hsa-miR-376a-3p	92
hsa-miR-199a-5p	92
hsa-miR-222-3p	90
hsa-miR-4286	89
hsa-miR-4516	70
hsa-miR-34a-5p	65
hsa-miR-1255a	64
hsa-miR-365a-3p+hsa-miR-365b-3p	63
hsa-miR-323a-3p	60
hsa-let-7c-5p	59

	Average counts
hsa-miR-27b-3p	58
hsa-miR-134-3p	57
hsa-miR-451a	52
hsa-miR-23b-3p	50
hsa-miR-423-5p	50
hsa-miR-28-5p	49
hsa-miR-125a-5p	49
hsa-miR-24-3p	49
hsa-miR-382-5p	48
hsa-miR-1228-3p	48
hsa-miR-20a-5p+hsa-miR-20b-5p	47
hsa-let-7e-5p	45
hsa-miR-18a-5p	43
hsa-miR-337-5p	43
hsa-miR-320e	42
hsa-miR-106a-5p+hsa-miR-17-5p	42
hsa-miR-19b-3p	41
hsa-miR-140-5p	40
hsa-let-7f-5p	39
hsa-miR-323a-5p	37
hsa-miR-148a-3p	35
hsa-miR-132-3p	32
hsa-miR-136-5p	30
hsa-miR-376c-3p	30
hsa-miR-379-5p	30
hsa-miR-26a-5p	29
hsa-miR-202-3p	29
hsa-miR-1290	29
hsa-miR-154-5p	27
hsa-miR-214-3p	27
hsa-miR-377-3p	27
hsa-miR-381-3p	25
hsa-miR-188-5p	25
hsa-miR-26b-5p	25
hsa-miR-363-3p	24
hsa-miR-337-3p	24
hsa-miR-137	23

Supplement Figure S3. MicroRNA transcript expression within explant-derived cell extracellular vesicles.

7.4 Human atrial extracellular vesicle or vehicle effects on atrial structure and fibrosis 3 days after surgery

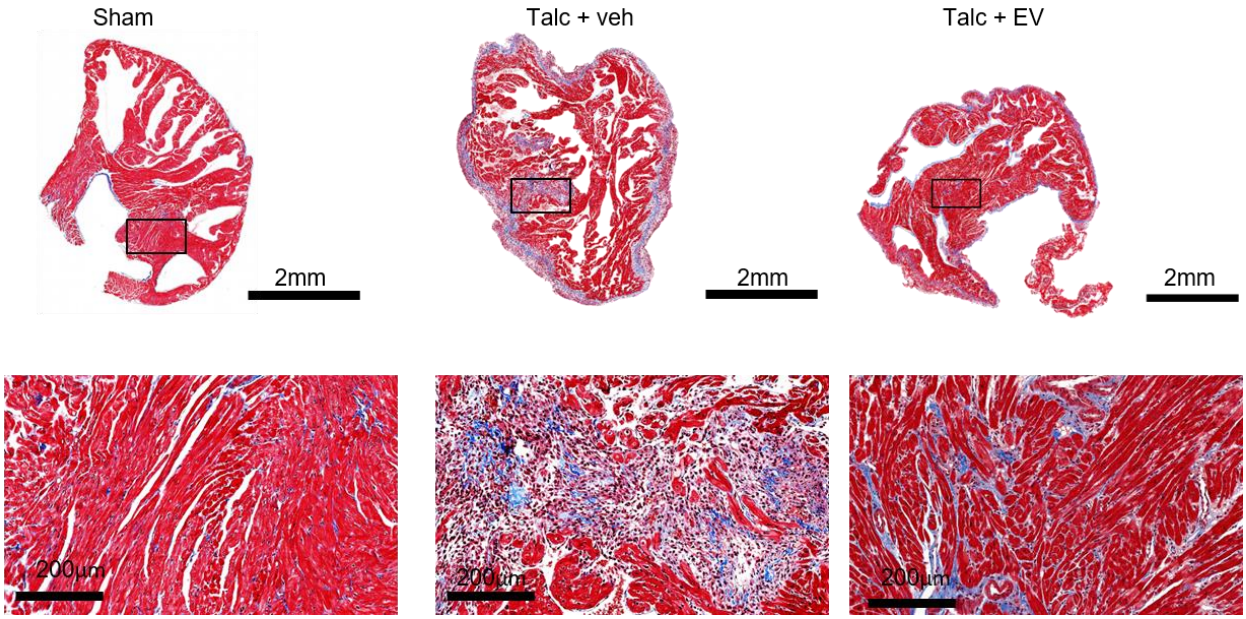

Supplement Figure S4. **Human atrial extracellular vesicle or vehicle effects on atrial structure and fibrosis 3 days after surgery.** Representative images of atrial tissue sections after Masson's Trichrome staining. Scale bar, 2 mm or 200 μm, as indicated.

7.5 Effect of explant-derived cell extracellular vesicles on inflammatory cells within the treated atria

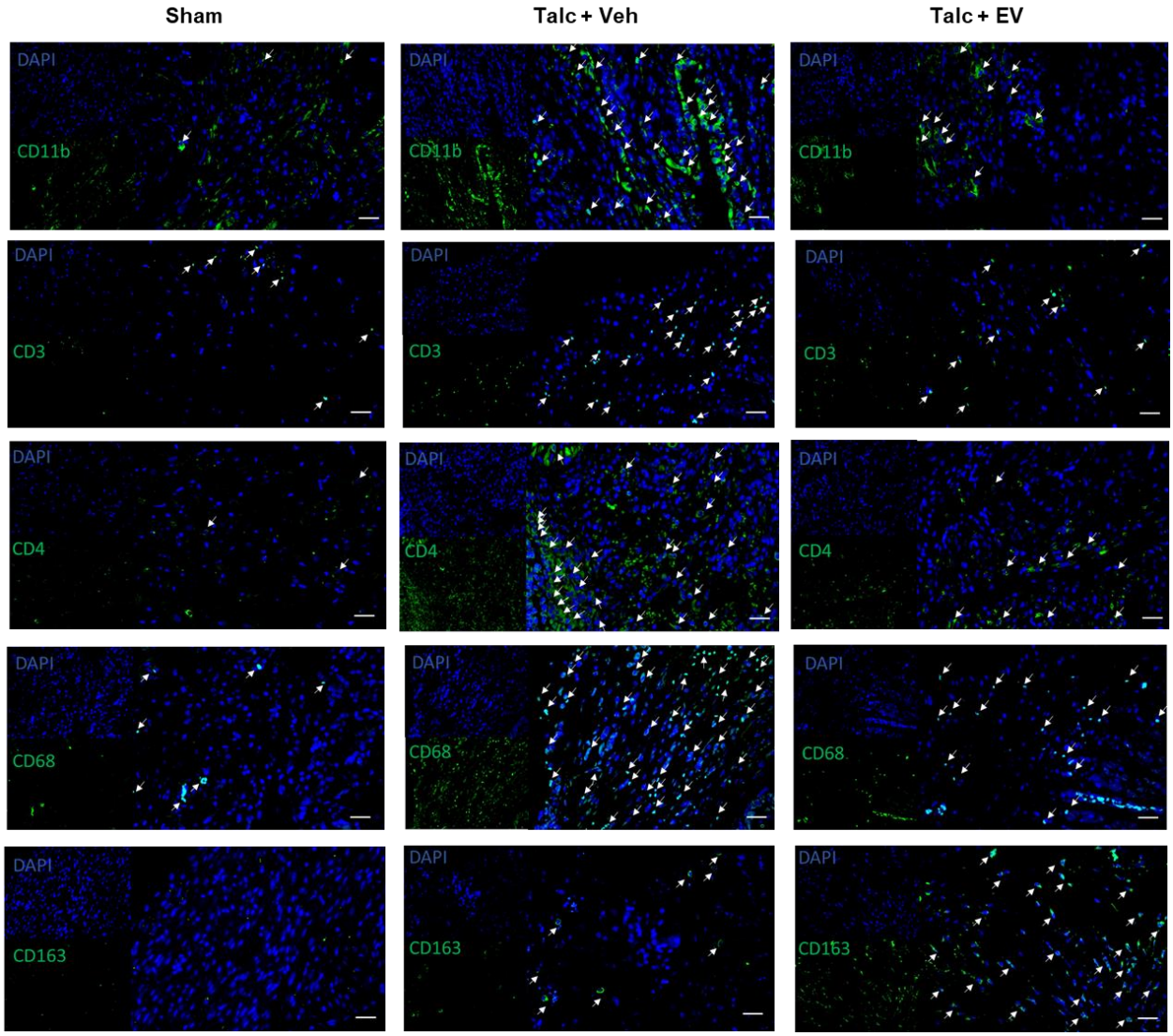

Supplement Figure S5. **Effect of explant-derived cell extracellular vesicles on inflammatory cells within the treated atria.** Representative images showing neutrophils (CD11b), cytotoxic T cells (CD3), T helper cells (CD4), pro-inflammatory M1 macrophages (CD68) and anti-inflammatory M2 macrophages (CD163 found within treated atria (n=5 biological replicates) after sham procedure, application of talc and vehicle (veh) or after application of talc and EVs. Positive cells are denoted with a white arrow. Scale bar 100 μM.

7.6 Human atrial extracellular vesicle or vehicle effects on atrial structure and fibrosis 7 days after surgery

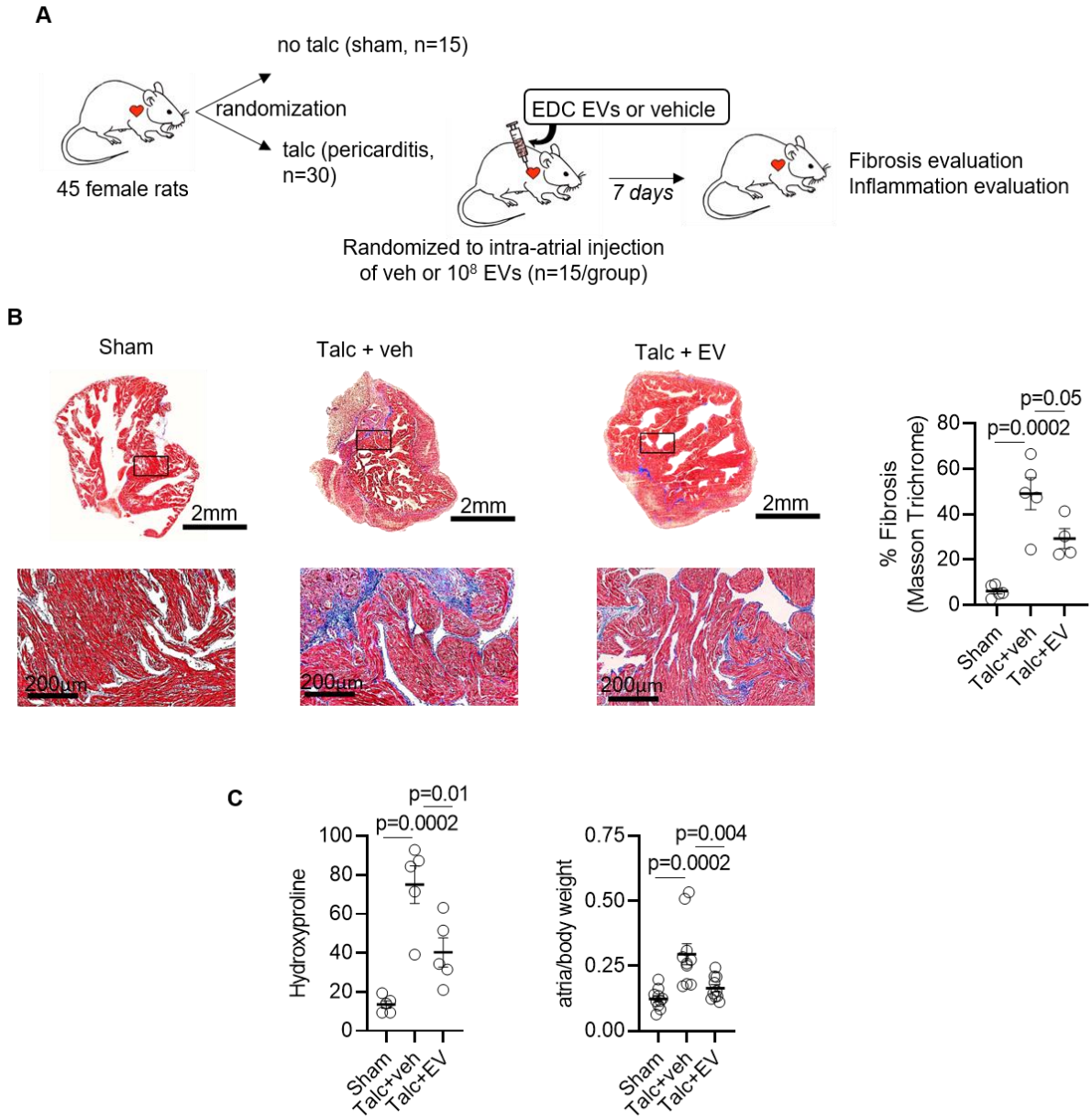

Supplement Figure S6. **Human atrial extracellular vesicle or vehicle effects on atrial structure and fibrosis 7 days after surgery. (A)** Study schematic demonstrating the study design, numbers of animals included, group allocations and outcomes measured. **(B)** Representative images of atrial tissue sections after Masson's Trichrome staining. Quantitative analysis showing

the effect of talc and EVs on inflammatory cell infiltration (n=5 biological replicates). **(C)** Effect of EV treatment on atrial fibrosis (n=5) and structure (n=5). One-way ANOVA with individual-mean comparisons by Bonferroni's multiple two-tailed comparisons test. Scale bar, 2 mm or 200 μm, as indicated.

7.7 Human atrial extracellular vesicle or vehicle effects on atrial inflammation days after surgery.

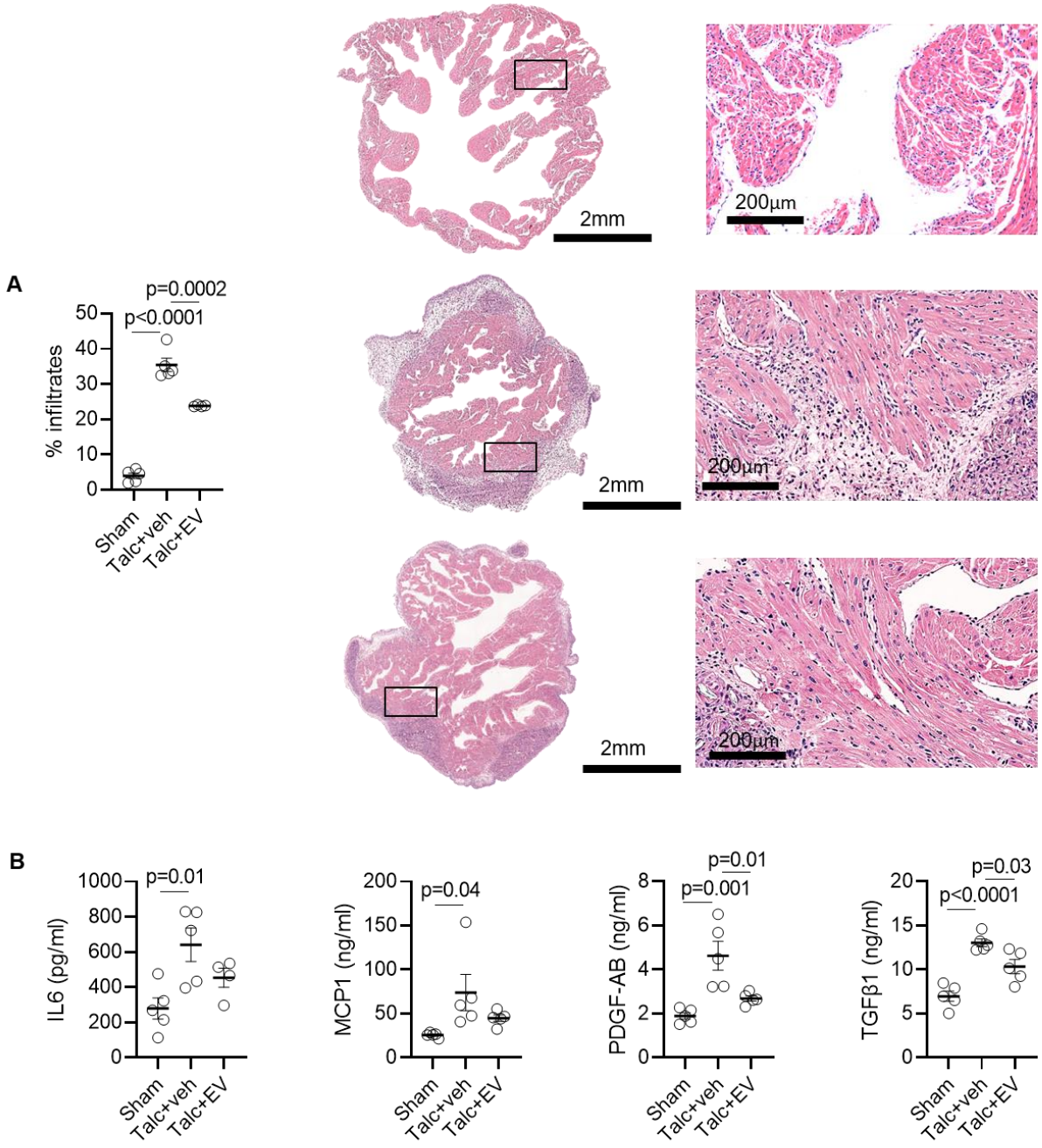

Supplement Figure S7. **Human atrial extracellular vesicle or vehicle effects on atrial inflammation days after surgery. (A)** Representative images of atrial tissue sections after hematoxylin and eosin staining showing the effect of talc and extracellular vesicles (EVs) on

inflammatory cell infiltration. Quantitative analysis showing the effect of talc and EVs on inflammatory cell infiltration (n=5 biological replicates). **(B)** Effect of talc and EVs on interleukin 6 (IL6), monocyte chemoattractant protein 1 (MCP1), platelet-derived growth factor AB (PDGF-AB) and transforming growth factor beta 1 (TGFβ1) expression (n=5 biological replicates). One-way ANOVA with individual-mean comparisons by Bonferroni's multiple two-tailed comparisons test. Scale bar, 2 mm or 200 μm, as indicated.

7.8 Effect of explant-derived cell extracellular vesicles on proliferation.

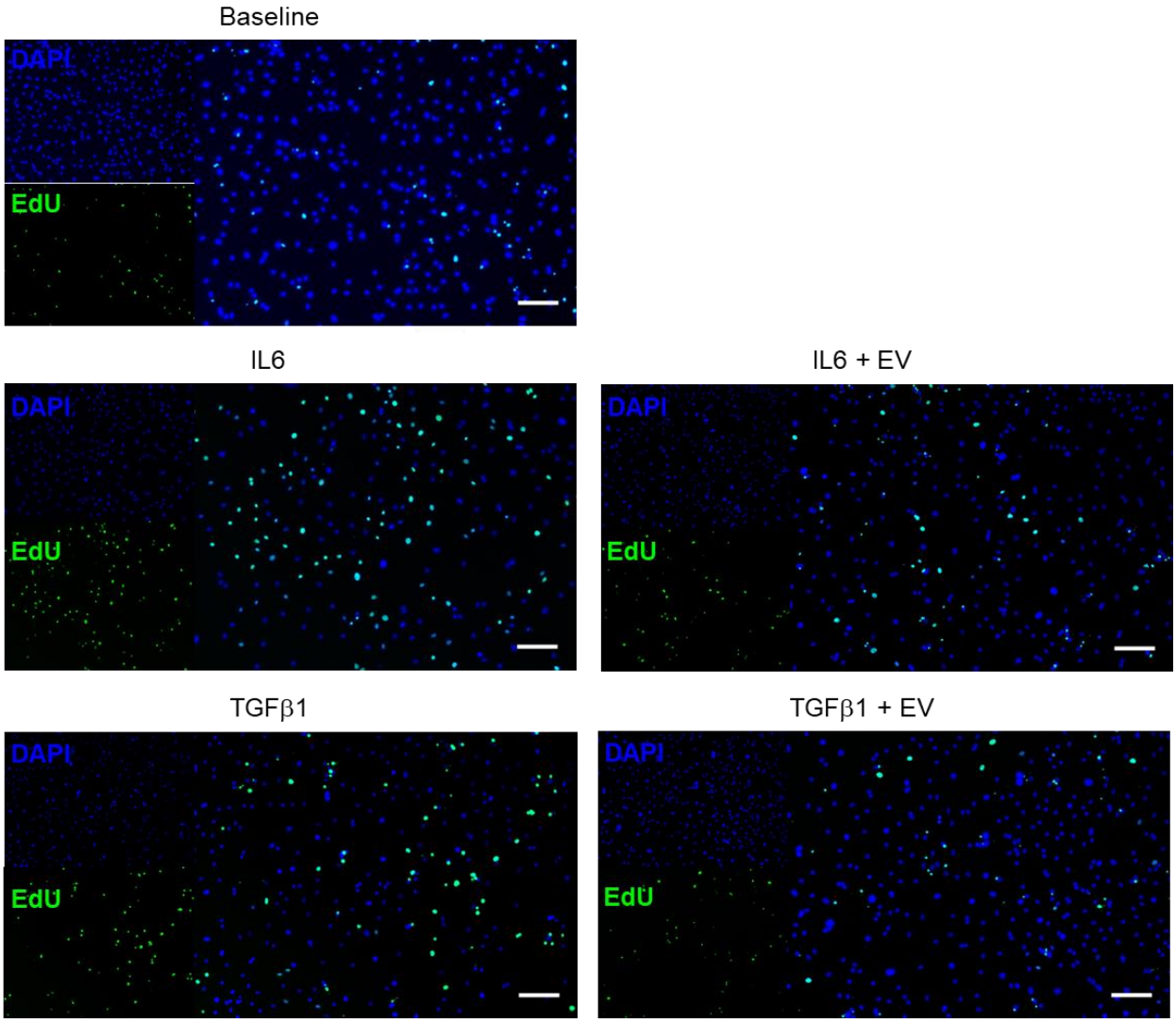

Supplement Figure S8. **Effect of explant-derived cell extracellular vesicles on proliferation.** Representative images showing 5-ethynyl-2´-deoxyuridine (EDU) and 4′,6-diamidino-2-phenylindole (DAPI) atrial fibroblasts at baseline and after treatment with interleukin 6 (IL6), transforming growth factor beta 1 (TGFβ1) and/or EDC EVs (n=5 biological replicates). Scale bar 200 μM

7.9 Effect of extracellular vesicles on electrocardiographic and electrophysiological function

	RR (ms)	PR (ms)	QRS (ms)	QT (ms)	AVERP (ms)
Female					
Sham	174±16	49±5	19±3	93±8	77±10
Talc + veh	163±17	48±3	18±3	87±12	76±11
Talc + EV	169±32	49±4	17±2	94±15	80±9
Male					
Sham	181±18	47±3	20±2	97±8	74±13
Talc + veh	157±12	46±4	18±2	88±9	76±10
Talc + EV	166±16	47±4	18±3	89±11	77±10

Supplement Table 1. **Effect of extracellular vesicles on electrocardiographic and electrophysiological function.** AVERP, atrioventricular nodal refractory period; EV, extracellular vesicles; veh, vehicle.

8.0 REFERENCES

1 Benjamin, E. J. *et al.* Independent risk factors for atrial fibrillation in a population-based cohort. The Framingham Heart Study. *Jama* **271**, 840-844 (1994).

2 Go, A. S. *et al.* Prevalence of diagnosed atrial fibrillation in adults: national implications for rhythm management and stroke prevention: the AnTicoagulation and Risk Factors in Atrial Fibrillation (ATRIA) Study. *Jama* **285**, 2370-2375 (2001). https://doi.org:10.1001/jama.285.18.2370

3 Furberg, C. D. *et al.* Prevalence of atrial fibrillation in elderly subjects (the Cardiovascular Health Study). *Am J Cardiol* **74**, 236-241 (1994). https://doi.org:10.1016/0002-9149(94)90363-8

4 Kaw, R. *et al.* Short- and long-term mortality associated with new-onset atrial fibrillation after coronary artery bypass grafting: a systematic review and meta-analysis. *J Thorac Cardiovasc Surg* **141**, 1305-1312 (2011). https://doi.org:10.1016/j.jtcvs.2010.10.040

5 LaPar, D. J. *et al.* Postoperative atrial fibrillation significantly increases mortality, hospital readmission, and hospital costs. *Ann Thorac Surg* **98**, 527-533; discussion 533 (2014). https://doi.org:10.1016/j.athoracsur.2014.03.039

6 Mathew, J. P. *et al.* A multicenter risk index for atrial fibrillation after cardiac surgery. *Jama* **291**, 1720-1729 (2004). https://doi.org:10.1001/jama.291.14.1720

7 Dobrev, D., Aguilar, M., Heijman, J., Guichard, J. B. & Nattel, S. Postoperative atrial fibrillation: mechanisms, manifestations and management. *Nat Rev Cardiol* **16**, 417-436 (2019). https://doi.org:10.1038/s41569-019-0166-5

8 Devereaux, P. J. *et al.* Effects of extended-release metoprolol succinate in patients undergoing non-cardiac surgery (POISE trial): a randomised controlled trial. *Lancet* **371**, 1839-1847 (2008). https://doi.org:10.1016/s0140-6736(08)60601-7

9 Arsenault, K. A. *et al.* Interventions for preventing post-operative atrial fibrillation in patients undergoing heart surgery. *Cochrane Database Syst Rev* **2013**, Cd003611 (2013). https://doi.org:10.1002/14651858.CD003611.pub3

10 Dieleman, J. M. *et al.* Intraoperative high-dose dexamethasone for cardiac surgery: a randomized controlled trial. *Jama* **308**, 1761-1767 (2012). https://doi.org:10.1001/jama.2012.14144

11 Whitlock, R. P. *et al.* Methylprednisolone in patients undergoing cardiopulmonary bypass (SIRS): a randomised, double-blind, placebo-controlled trial. *Lancet* **386**, 1243-1253 (2015). https://doi.org:10.1016/s0140-6736(15)00273-1

12 Seo, C., Michie, C., Hibbert, B. & Davis, D. R. Systematic review of pre-clinical therapies for post-operative atrial fibrillation. *PLoS One* **15**, e0241643 (2020). https://doi.org:10.1371/journal.pone.0241643

13 McRae, C., Kapoor, A., Kanda, P., Hibbert, B. & Davis, D. R. Systematic review of biological therapies for atrial fibrillation. *Heart Rhythm* **16**, 1399-1407 (2019). https://doi.org:10.1016/j.hrthm.2019.03.021

14 Marbán, E. The Secret Life of Exosomes: What Bees Can Teach Us About Next-Generation Therapeutics. *J Am Coll Cardiol* **71**, 193-200 (2018). https://doi.org:10.1016/j.jacc.2017.11.013

15 Aminzadeh, M. A. *et al.* Exosome-Mediated Benefits of Cell Therapy in Mouse and Human Models of Duchenne Muscular Dystrophy. *Stem Cell Reports* **10**, 942-955 (2018). https://doi.org:10.1016/j.stemcr.2018.01.023

16 de Couto, G. *et al.* Exosomal MicroRNA Transfer Into Macrophages Mediates Cellular Postconditioning. *Circulation* **136**, 200-214 (2017). https://doi.org:10.1161/circulationaha.116.024590

17 Gallet, R. *et al.* Exosomes secreted by cardiosphere-derived cells reduce scarring, attenuate adverse remodelling, and improve function in acute and chronic porcine myocardial infarction. *Eur Heart J* **38**, 201-211 (2017). https://doi.org:10.1093/eurheartj/ehw240

18 Tseliou, E. *et al.* Fibroblasts Rendered Antifibrotic, Antiapoptotic, and Angiogenic by Priming With Cardiosphere-Derived Extracellular Membrane Vesicles. *J Am Coll Cardiol* **66**, 599-611 (2015). https://doi.org:10.1016/j.jacc.2015.05.068

19 Ibrahim, A. G., Cheng, K. & Marbán, E. Exosomes as critical agents of cardiac regeneration triggered by cell therapy. *Stem Cell Reports* **2**, 606-619 (2014). https://doi.org:10.1016/j.stemcr.2014.04.006

20 Huang, Z. *et al.* Signal Transducer and Activator of Transcription 3/MicroRNA-21 Feedback Loop Contributes to Atrial Fibrillation by Promoting Atrial Fibrosis in a Rat Sterile Pericarditis Model. *Circ Arrhythm Electrophysiol* **9**, e003396 (2016). https://doi.org:10.1161/circep.115.003396

21 Mount, S. *et al.* Physiologic expansion of human heart-derived cells enhances therapeutic repair of injured myocardium. *Stem Cell Res Ther* **10**, 316 (2019). https://doi.org:10.1186/s13287-019-1418-3

22 Lalu, M. M. *et al.* Safety of cell therapy with mesenchymal stromal cells (SafeCell): a systematic review and meta-analysis of clinical trials. *PLoS One* **7**, e47559 (2012). https://doi.org:10.1371/journal.pone.0047559

23 Mayfield, A. E. *et al.* The impact of patient co-morbidities on the regenerative capacity of cardiac explant-derived stem cells. *Stem Cell Res Ther* **7**, 60 (2016). https://doi.org:10.1186/s13287-016-0321-4

24 Molgat, A. S. *et al.* Hyperglycemia inhibits cardiac stem cell-mediated cardiac repair and angiogenic capacity. *Circulation* **130**, S70-76 (2014). https://doi.org:10.1161/circulationaha.113.007908

25 Davis, D. R. *et al.* Isolation and expansion of functionally-competent cardiac progenitor cells directly from heart biopsies. *J Mol Cell Cardiol* **49**, 312-321 (2010). https://doi.org:10.1016/j.yjmcc.2010.02.019

26 Latham, N. *et al.* Human blood and cardiac stem cells synergize to enhance cardiac repair when cotransplanted into ischemic myocardium. *Circulation* **128**, S105-112 (2013). https://doi.org:10.1161/circulationaha.112.000374

27 Li, T. S. *et al.* Expansion of human cardiac stem cells in physiological oxygen improves cell production efficiency and potency for myocardial repair. *Cardiovasc Res* **89**, 157-165 (2011). https://doi.org:10.1093/cvr/cvq251

28 Villanueva, M. *et al.* Glyoxalase 1 Prevents Chronic Hyperglycemia Induced Heart-Explant Derived Cell Dysfunction. *Theranostics* **9**, 5720-5730 (2019). https://doi.org:10.7150/thno.36639

29 Kanda, P. *et al.* Deterministic Encapsulation of Human Cardiac Stem Cells in Variable Composition Nanoporous Gel Cocoons To Enhance Therapeutic Repair of Injured Myocardium. *ACS Nano* **12**, 4338-4350 (2018). https://doi.org:10.1021/acsnano.7b08881

30 Risha, Y., Minic, Z., Ghobadloo, S. M. & Berezovski, M. V. The proteomic analysis of breast cell line exosomes reveals disease patterns and potential biomarkers. *Sci Rep* **10**, 13572 (2020). https://doi.org:10.1038/s41598-020-70393-4

31 Sidiropoulos, K. *et al.* Reactome enhanced pathway visualization. *Bioinformatics* **33**, 3461-3467 (2017). https://doi.org:10.1093/bioinformatics/btx441

32 Welsh, J. A., Jones, J. C. & Tang, V. A. Fluorescence and Light Scatter Calibration Allow Comparisons of Small Particle Data in Standard Units across Different Flow Cytometry Platforms and Detector Settings. *Cytometry A* **97**, 592-601 (2020). https://doi.org:10.1002/cyto.a.24029

33 Welsh, J. A. & Jones, J. C. Small Particle Fluorescence and Light Scatter Calibration Using FCMPASS Software. *Curr Protoc Cytom* **94**, e79 (2020). https://doi.org:10.1002/cpcy.79

34 Consortium, E.-T. *et al.* EV-TRACK: transparent reporting and centralizing knowledge in extracellular vesicle research. *Nat Methods* **14**, 228-232 (2017). https://doi.org:10.1038/nmeth.4185

35 Cardin, S. *et al.* Role for MicroRNA-21 in atrial profibrillatory fibrotic remodeling associated with experimental postinfarction heart failure. *Circ Arrhythm Electrophysiol* **5**, 1027-1035 (2012). https://doi.org:10.1161/circep.112.973214

36 Kapoor, N., Liang, W., Marbán, E. & Cho, H. C. Direct conversion of quiescent cardiomyocytes to pacemaker cells by expression of Tbx18. *Nat Biotechnol* **31**, 54-62 (2013). https://doi.org:10.1038/nbt.2465

37 El Harane, N. *et al.* Acellular therapeutic approach for heart failure: in vitro production of extracellular vesicles from human cardiovascular progenitors. *Eur Heart J* **39**, 1835-1847 (2018). https://doi.org:10.1093/eurheartj/ehy012

38 Gray, A., Wright, A., Jackson, P., Hale, M. & Treanor, D. Quantification of histochemical stains using whole slide imaging: development of a method and demonstration of its usefulness in laboratory quality control. *J Clin Pathol* **68**, 192-199 (2015). https://doi.org:10.1136/jclinpath-2014-202526

39 He, X. *et al.* Atrial fibrillation induces myocardial fibrosis through angiotensin II type 1 receptor-specific Arkadia-mediated downregulation of Smad7. *Circ Res* **108**, 164-175 (2011). https://doi.org:10.1161/circresaha.110.234369

40 Jamall, I. S., Finelli, V. N. & Que Hee, S. S. A simple method to determine nanogram levels of 4-hydroxyproline in biological tissues. *Anal Biochem* **112**, 70-75 (1981). https://doi.org:10.1016/0003-2697(81)90261-x

41 Narikawa, M. *et al.* Acute Hyperthermia Inhibits TGF-β1-induced Cardiac Fibroblast Activation via Suppression of Akt Signaling. *Sci Rep* **8**, 6277 (2018). https://doi.org:10.1038/s41598-018-24749-6

42 Lötvall, J. *et al.* Minimal experimental requirements for definition of extracellular vesicles and their functions: a position statement from the International Society for Extracellular Vesicles. *J Extracell Vesicles* **3**, 26913 (2014). https://doi.org:10.3402/jev.v3.26913

43 Girmatsion, Z. *et al.* Changes in microRNA-1 expression and IK1 up-regulation in human atrial fibrillation. *Heart Rhythm* **6**, 1802-1809 (2009). https://doi.org:10.1016/j.hrthm.2009.08.035

44 Tsoporis, J. N. *et al.* Increased right atrial appendage apoptosis is associated with differential regulation of candidate MicroRNAs 1 and 133A in patients who developed atrial fibrillation after cardiac surgery. *J Mol Cell Cardiol* **121**, 25-32 (2018). https://doi.org:10.1016/j.yjmcc.2018.06.005

45 Small, E. M., Frost, R. J. & Olson, E. N. MicroRNAs add a new dimension to cardiovascular disease. *Circulation* **121**, 1022-1032 (2010). https://doi.org:10.1161/circulationaha.109.889048

46 Shan, H. *et al.* Downregulation of miR-133 and miR-590 contributes to nicotine-induced atrial remodelling in canines. *Cardiovasc Res* **83**, 465-472 (2009). https://doi.org:10.1093/cvr/cvp130

47 Luo, X. *et al.* MicroRNA-26 governs profibrillatory inward-rectifier potassium current changes in atrial fibrillation. *J Clin Invest* **123**, 1939-1951 (2013). https://doi.org:10.1172/jci62185

48 van Rooij, E. *et al.* Dysregulation of microRNAs after myocardial infarction reveals a role of miR-29 in cardiac fibrosis. *Proc Natl Acad Sci U S A* **105**, 13027-13032 (2008). https://doi.org:10.1073/pnas.0805038105

49 Lim, L. H., Solito, E., Russo-Marie, F., Flower, R. J. & Perretti, M. Promoting detachment of neutrophils adherent to murine postcapillary venules to control inflammation: effect of lipocortin 1. *Proc Natl Acad Sci U S A* **95**, 14535-14539 (1998). https://doi.org:10.1073/pnas.95.24.14535

50 Vital, S. A. *et al.* Formyl-Peptide Receptor 2/3/Lipoxin A4 Receptor Regulates Neutrophil-Platelet Aggregation and Attenuates Cerebral Inflammation: Impact for Therapy in

Cardiovascular Disease. *Circulation* **133**, 2169-2179 (2016). https://doi.org:10.1161/circulationaha.115.020633

51 de Jong, R. C. M. *et al.* Annexin A5 reduces infarct size and improves cardiac function after myocardial ischemia-reperfusion injury by suppression of the cardiac inflammatory response. *Sci Rep* **8**, 6753 (2018). https://doi.org:10.1038/s41598-018-25143-y

52 Burgmaier, M. *et al.* AnxA5 reduces plaque inflammation of advanced atherosclerotic lesions in apoE(-/-) mice. *J Cell Mol Med* **18**, 2117-2124 (2014). https://doi.org:10.1111/jcmm.12374

53 Ewing, M. M. *et al.* Annexin A5 therapy attenuates vascular inflammation and remodeling and improves endothelial function in mice. *Arterioscler Thromb Vasc Biol* **31**, 95-101 (2011). https://doi.org:10.1161/atvbaha.110.216747

54 Jung, J. Y. *et al.* Protective effect of hemopexin on systemic inflammation and acute lung injury in an endotoxemia model. *J Surg Res* **212**, 15-21 (2017). https://doi.org:10.1016/j.jss.2016.12.020

55 Liang, X. *et al.* Hemopexin down-regulates LPS-induced proinflammatory cytokines from macrophages. *J Leukoc Biol* **86**, 229-235 (2009). https://doi.org:10.1189/jlb.1208742

56 Correa, S. G., Sotomayor, C. E., Aoki, M. P., Maldonado, C. A. & Rabinovich, G. A. Opposite effects of galectin-1 on alternative metabolic pathways of L-arginine in resident, inflammatory, and activated macrophages. *Glycobiology* **13**, 119-128 (2003). https://doi.org:10.1093/glycob/cwg010

57 Canesi, F. *et al.* A thioredoxin-mimetic peptide exerts potent anti-inflammatory, antioxidant, and atheroprotective effects in ApoE2.Ki mice fed high fat diet. *Cardiovasc Res* **115**, 292-301 (2019). https://doi.org:10.1093/cvr/cvy183

58 El Hadri, K. *et al.* Thioredoxin-1 promotes anti-inflammatory macrophages of the M2 phenotype and antagonizes atherosclerosis. *Arterioscler Thromb Vasc Biol* **32**, 1445-1452 (2012). https://doi.org:10.1161/atvbaha.112.249334

59 Baghy, K., Iozzo, R. V. & Kovalszky, I. Decorin-TGFβ axis in hepatic fibrosis and cirrhosis. *J Histochem Cytochem* **60**, 262-268 (2012). https://doi.org:10.1369/0022155412438104

60 Parichatikanond, W., Luangmonkong, T., Mangmool, S. & Kurose, H. Therapeutic Targets for the Treatment of Cardiac Fibrosis and Cancer: Focusing on TGF-β Signaling. *Front Cardiovasc Med* **7**, 34 (2020). https://doi.org:10.3389/fcvm.2020.00034

61 Onozuka, I. *et al.* Cholestatic liver fibrosis and toxin-induced fibrosis are exacerbated in matrix metalloproteinase-2 deficient mice. *Biochem Biophys Res Commun* **406**, 134-140 (2011). https://doi.org:10.1016/j.bbrc.2011.02.012

62 Radbill, B. D. *et al.* Loss of matrix metalloproteinase-2 amplifies murine toxin-induced liver fibrosis by upregulating collagen I expression. *Dig Dis Sci* **56**, 406-416 (2011). https://doi.org:10.1007/s10620-010-1296-0

63 Roberts, W. C. Pericardial heart disease: its morphologic features and its causes. *Proc (Bayl Univ Med Cent)* **18**, 38-55 (2005). https://doi.org:10.1080/08998280.2005.11928030

64 Yue, L., Xie, J. & Nattel, S. Molecular determinants of cardiac fibroblast electrical function and therapeutic implications for atrial fibrillation. *Cardiovasc Res* **89**, 744-753 (2011). https://doi.org:10.1093/cvr/cvq329

65 Aguilar, M., Heijman, J., Dobrev, D. & Nattel, S. One Ring to Rule Them All: Continuous Monitoring of Patients With Secondary Atrial Fibrillation Points to a Unifying Underlying Mechanism. *Can J Cardiol* **37**, 686-689 (2021). https://doi.org:10.1016/j.cjca.2021.01.018

66 de Couto, G. *et al.* Macrophages mediate cardioprotective cellular postconditioning in acute myocardial infarction. *J Clin Invest* **125**, 3147-3162 (2015). https://doi.org:10.1172/jci81321

67 Heijman, J. *et al.* Atrial Myocyte NLRP3/CaMKII Nexus Forms a Substrate for Postoperative Atrial Fibrillation. *Circ Res* **127**, 1036-1055 (2020). https://doi.org:10.1161/circresaha.120.316710

68 Fu, X. X. *et al.* Interleukin-17A contributes to the development of post-operative atrial fibrillation by regulating inflammation and fibrosis in rats with sterile pericarditis. *Int J Mol Med* **36**, 83-92 (2015). https://doi.org:10.3892/ijmm.2015.2204

69 Hooijmans, C. R. *et al.* SYRCLE's risk of bias tool for animal studies. *BMC Med Res Methodol* **14**, 43 (2014). https://doi.org:10.1186/1471-2288-14-43

70 Macleod, M. R., O'Collins, T., Howells, D. W. & Donnan, G. A. Pooling of animal experimental data reveals influence of study design and publication bias. *Stroke* **35**, 1203-1208 (2004). https://doi.org:10.1161/01.Str.0000125719.25853.20

71 Soucek, R. *et al.* Genetic suppression of atrial fibrillation using a dominant-negative ether-a-go-go-related gene mutant. *Heart Rhythm* **9**, 265-272 (2012). https://doi.org:10.1016/j.hrthm.2011.09.008

72 Amit, G. *et al.* Selective molecular potassium channel blockade prevents atrial fibrillation. *Circulation* **121**, 2263-2270 (2010). https://doi.org:10.1161/circulationaha.109.911156

73 Liu, Z. *et al.* Preclinical efficacy and safety of KCNH2-G628S gene therapy for postoperative atrial fibrillation. *J Thorac Cardiovasc Surg* **154**, 1644-1651.e1648 (2017). https://doi.org:10.1016/j.jtcvs.2017.05.052

74 Perlstein, I. *et al.* Posttranslational control of a cardiac ion channel transgene in vivo: clarithromycin-hMiRP1-Q9E interactions. *Hum Gene Ther* **16**, 906-910 (2005). https://doi.org:10.1089/hum.2005.16.906

75 Jia, X. *et al.* MicroRNA-1 accelerates the shortening of atrial effective refractory period by regulating KCNE1 and KCNB2 expression: an atrial tachypacing rabbit model. *PLoS One* **8**, e85639 (2013). https://doi.org:10.1371/journal.pone.0085639

76 Lugenbiel, P. *et al.* TREK-1 (K(2P)2.1) K(+) channels are suppressed in patients with atrial fibrillation and heart failure and provide therapeutic targets for rhythm control. *Basic Res Cardiol* **112**, 8 (2017). https://doi.org:10.1007/s00395-016-0597-7